ORIGINAL RESEARCH

The Regulation of Fatty Acid Synthase by Exosomal miR-143-5p and miR-342-5p in Idiopathic Pulmonary Fibrosis

Hassan Hayek[1,2], Ohoud Rehbini[2], Beata Kosmider[1,2,3], Thomas Brandt[2], Wissam Chatila[3], Nathaniel Marchetti[3], Gerard J. Criner[3], Sudhir Bolla[3], Raj Kishore[4,5], Russell P. Bowler[6], and Karim Bahmed[1,2,3]

[1]Department of Microbiology, Immunology, and Inflammation, [2]Center for Inflammation and Lung Research, [3]Department of Thoracic Medicine and Surgery, [4]Center for Translational Medicine, and [5]Department of Cardiovascular Sciences, Temple University, Philadelphia, Pennsylvania; and [6]Department of Medicine, National Jewish Health, Denver, Colorado

ORCID ID: 0000-0003-4651-363X (R.P.B.).

Abstract

Idiopathic pulmonary fibrosis (IPF) is a chronic and progressive disease caused by an aberrant repair of injured alveolar epithelial cells. The maintenance of the alveolar epithelium and its regeneration after the damage is fueled by alveolar type II (ATII) cells. Injured cells release exosomes containing microRNAs (miRNAs), which can alter the recipient cells' function. Lung tissue, ATII cells, fibroblasts, plasma, and exosomes were obtained from naive patients with IPF, patients with IPF taking pirfenidone or nintedanib, and control organ donors. miRNA expression was analyzed to study their impact on exosome-mediated effects in IPF. High miR-143-5p and miR-342-5p levels were detected in ATII cells, lung tissue, plasma, and exosomes in naive patients with IPF. Decreased FASN (fatty acid synthase) and ACSL-4 (acyl-CoA-synthetase long-chain family member 4) expression was found in ATII cells. miR-143-5p and miR-342-5p overexpression or ATII cell treatment with IPF-derived exosomes containing these miRNAs lowered FASN and ACSL-4 levels. Also, this contributed to ATII cell injury and senescence. However, exosomes isolated from patients with IPF taking nintedanib or pirfenidone increased FASN expression in ATII cells compared with naive patients with IPF. Furthermore, fibroblast treatment with exosomes obtained from naive patients with IPF increased SMAD3, CTGF, COL3A1, and TGFβ1 expression. Our results suggest that IPF-derived exosomes containing miR-143-5p and miR-342-5p inhibited the *de novo* fatty acid synthesis pathway in ATII cells. They also induced the profibrotic response in fibroblasts. Pirfenidone and nintedanib improved ATII cell function and inhibited fibrogenesis. This study highlights the importance of exosomes in IPF pathophysiology.

Keywords: exosomes; microRNA; alveolar type II cells; fatty acid synthesis; IPF

Idiopathic pulmonary fibrosis (IPF) is a chronic interstitial lung disease of unknown etiology, usually diagnosed in patients more than 50 years old (1). This disease is characterized by scarring of lung tissue, leading to the destruction of the lung architecture and respiratory failure (2). Pirfenidone and nintedanib improve the clinical prognosis; however, their mechanism of action is still not well understood (3).

Alveolar type II (ATII) cells have stem cell potential and are characterized by the ability of self-renewal and differentiation to alveolar type I cells after injury (4). They produce and release pulmonary surfactants to reduce surface tension and prevent the alveoli from collapsing. The main features of IPF at the cellular level include alveolar epithelium injury with the loss of ATII cells and their regenerative capacity (5). Notably, a study shows a potential beneficial effect of ATII cell transplantation in IPF (6).

Exosomes are one subtype of vesicles (30–150 nm) constitutively secreted by

(Received in original form June 27, 2023; accepted in final form December 19, 2023)

Supported by National Institutes of Health grants HL134608 (R.K.), R01 ES032081 (B.K.), R01 HL150587 (B.K.), and R21 ES030808 (K.B.), and U.S. Department of Defense grants W81XWH2110400 (K.B.) and W81XWH2110414 (B.K.) and discretionary funds from Temple University (B.K. and K.B.).

Author Contributions: H.H., O.R., B.K., and T.B. conducted experiments and/or contributed to data analysis and manuscript writing. W.C., N.M., G.J.C., S.B., R.K., and R.P.B. provided critical reagents and resources, analyzed data, and contributed to manuscript writing. K.B. provided funding acquisition, project administration, supervision, data analysis, and manuscript writing.

Correspondence and requests for reprints should be addressed to Karim Bahmed, Ph.D., Department of Microbiology, Immunology, and Inflammation, Center for Inflammation and Lung Research, Temple University, 3500 North Broad Street, Philadelphia, PA 19140. E-mail: karim.bahmed@temple.edu.

This article has a related editorial.

This article has a data supplement, which is accessible at the Supplements tab.

Am J Respir Cell Mol Biol Vol 70, Iss 4, pp 259–282, April 2024

Originally Published in Press as DOI: 10.1165/rcmb.2023-0232OC on December 20, 2023
Internet address: www.atsjournals.org

Table 1. Baseline Characteristics of Organ Donors and Patients with IPF

Characteristic	Control Subjects	IPF	Medicated		*P* Value*
			Nintedanib	Pirfenidone	
n	30	13	7	9	—
Age, yr, mean ± SEM	63.13 ± 1.73	62.76 ± 2.41	68.28 ± 2	70.22 ± 1.23	0.0894
Sex, *n* (%)	11 M (36.66) 18 F (60)	10 M (76.92) 3 F (23.08)	5 M (71.43) 2 F (28.57)	8 M (88.89) 1 F (11.11)	0.3778 0.2157
Ethnicity, *n* (%)					
White	21 (70)	9 (69.23)	6 (85.71)	9 (100)	0.9151
African American	4 (13.33)	3 (23.08)	1 (14.29)	0	0.7947
Hispanic	2 (6.66)	0	0	0	—
Asian	0	1 (7.69)	0	0	—
Lung function, mean ± SEM					
FVC, L	n/a	1.73 ± 0.21	2.23 ± 0.32	2.38 ± 0.42	0.1810
FVC % predicted	n/a	41 ± 4.57	56.28 ± 7.71	49.87 ± 3.94	0.1743
FEV_1, L	n/a	1.46 ± 0.19	1.76 ± 0.25	1.70 ± 0.20	0.3942
FEV_1% predicted	n/a	42.84 ± 4.96	60.14 ± 8.04	54.75 ± 4.41	0.0701
FEV_1/FVC, %	n/a	81.05 ± 3.42	80 ± 1.23	80.25 ± 1.09	0.3663

Definition of abbreviations: FEV_1 = forced expiratory volume in 1 second; FVC = forced vital capacity; IPF = idiopathic pulmonary fibrosis; n/a = not applicable.
*Testing for a difference between groups using Kruskal-Wallis and chi-square tests.

cells (7). Cell-derived exosome cargoes are loaded with nucleic acids and proteins, which can be delivered to neighboring cells (8). Exosome content is protected from degradation because of the presence of lipid bilayers (9). The involvement of exosomes and lung cell–derived extracellular vesicles (EVs) in pulmonary fibrosis pathophysiology was previously reported (10, 11). Kadota and colleagues found that EVs derived from human bronchial epithelial cells attenuated this disease by inhibiting TGF-β–WNT cross-talk (12). Fibroblast-derived EV obtained from patients with IPF induced cellular senescence via EV-mediated transfer of pathogenic cargo to lung epithelial cells (13).

Among cell-derived exosome cargoes, microRNAs (miRNAs) are the most extensively studied (14). Their roles in health and disease are established, and increasing clinical and experimental evidence implicates their dysregulated expression in lung diseases (15). Profibrotic and antifibrotic miRNAs' function in IPF was demonstrated (16). Moreover, we have recently reported the role of miRNA-200 family members in ATII cells in IPF (17).

Here, we performed *in silico* analysis, which indicated that miR-143-5p and miR-342-5p target the *de novo* fatty acid synthesis pathway, affecting fundamental cellular processes, including signal transduction and gene expression (18). This pathway involves FASN (fatty acid synthase) and ACSL-4 (acyl-CoA-synthetase long-chain family member 4) enzymes. FASN is the only human lipogenic enzyme that catalyzes the endogenous synthesis of fatty acids (19). Studies demonstrated that FASN is a critical protein in fatty acid synthesis in several diseases (20, 21). Notably, the reduced FASN expression contributed to acute lung injury in mice (22). Furthermore, emerging evidence suggests that the fatty acid synthesis pathway regulates cell proliferation and senescence (23).

We investigated the effect of exosomes obtained from patients with IPF on ATII cells isolated from control organ donors. To our knowledge, this is the first report on the role of miR-143-5p and miR-342-5p in FASN- and ACSL-4–mediated modulation of ATII cell function in this disease.

Methods

Human Lungs

Lungs were obtained from control organ donors without evidence of any respiratory diseases through the Gift of Life Donor Program (Philadelphia, PA) and IPF transplants (Temple University). Demographic and clinical characteristics are shown in Tables 1 and E1 in the data supplement. ATII cells were isolated, as we previously described (24). Fresh frozen plasma from EDTA tubes was used, as we reported (25). All participants signed written informed consent. The study was approved by the Temple University and National Jewish Health Institutional Review Boards.

Exosome Isolation

Exosomes were isolated from human plasma and lung tissue obtained from control organ donors and patients with IPF using ultracentrifugation (26).

Cell Analysis

Freshly isolated ATII cells were fixed in 1% glutaraldehyde and 4% paraformaldehyde. Sections were examined in a JEOL 1010 electron microscope, and digital images were recorded with a Hamamatsu camera system. Immunofluorescence, hematoxylin and eosin, and Masson's trichrome staining and wound-healing assays were performed.

Cell Transfection with miRNA Mimics

Control cultured ATII cells and fibroblasts were transfected with 20 nM of nontarget miRNA, miR-143-5p, or miR-342-5p mimics for 24 hours using Lipofectamine RNAiMAX Transfection Reagent (Invitrogen) according to the manufacturer's protocol.

Chest Computed Tomography

The Temple Lung Center Biobank collects lung tissue and associated clinical data from patients who provide informed consent to store their deidentified data and tissue for research purposes. High-resolution computed tomography scans were obtained as part of routine clinical care before

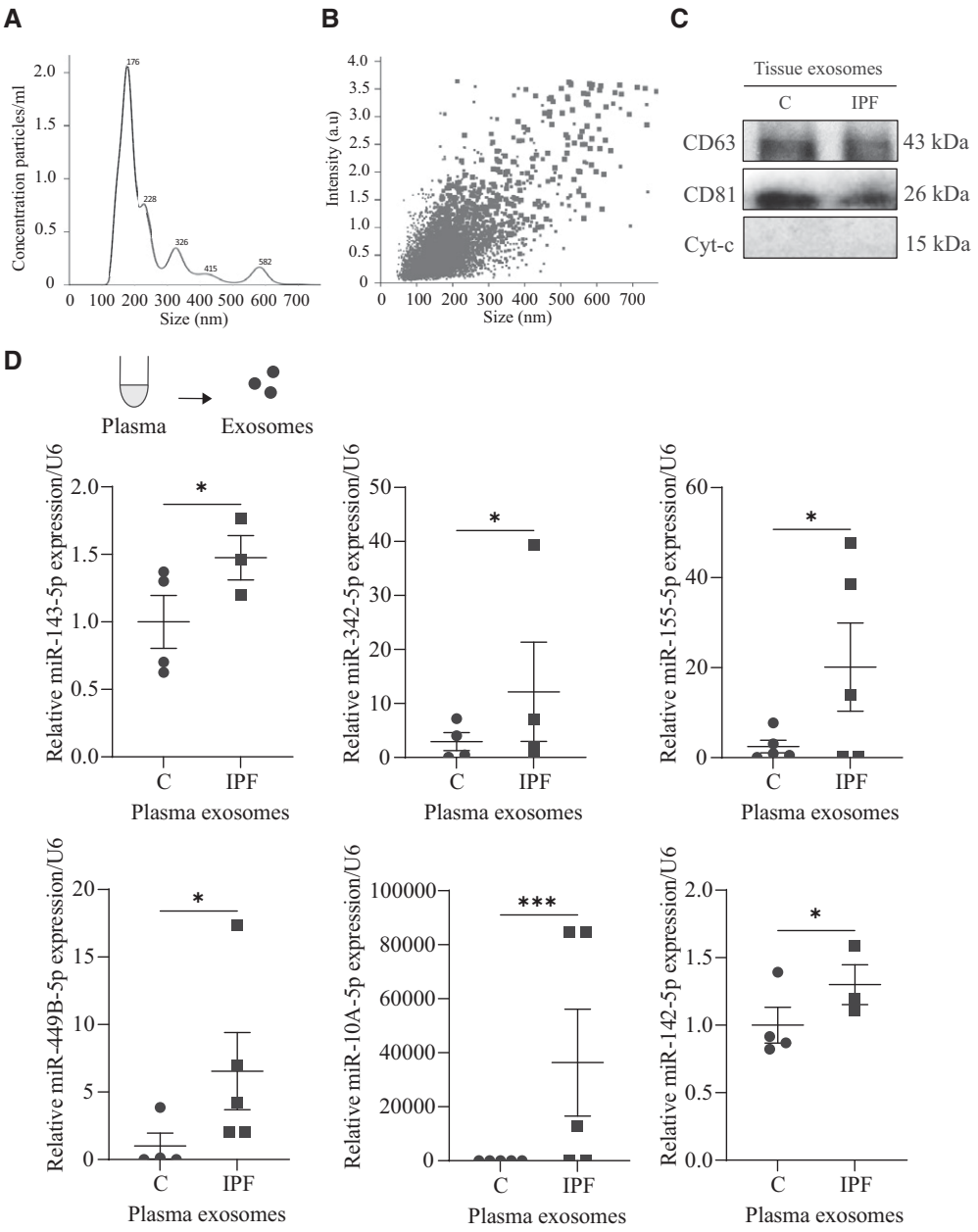

Figure 1. Characterization and identification of exosomes. Exosomes were isolated from lung tissue and plasma obtained from control organ donors (C) and naive patients with idiopathic pulmonary fibrosis (IPF). (*A*) Representative diagram of size and concentration of lung tissue–derived exosomes using NanoSight. (*B*) Representative diagram of lung tissue–derived exosomes analyzed by NanoSight. (*C*) Western blot images of CD63, CD81, and Cyt-c (cytochrome c) expression in lung tissue–derived exosomes. (*D*) microRNA (miRNA) levels were determined in exosomes obtained from plasma using RT-PCR. (*E*) miRNA expression in plasma by RT-PCR. ($N = 3$–7 samples per group. $^{*}P < 0.05$, $^{**}P < 0.01$, and $^{***}P < 0.001$.) Data are shown as means ± SEM.

transplant, and the scans were used to identify areas in the lung to sample.

RT-PCR

Total RNA from exosomes, cells, and lung tissue was obtained using Qiazol reagent (Qiagen Sciences) and miRNeasy kit (Qiagen) per the manufacturer's instructions, followed by RT-PCR.

Western Blotting

Lung tissue was homogenized using buffer with protease and phosphatase inhibitor cocktail (Gold Biotechnology), separated using 8–16% polyacrylamide gradient gels (Thermo Fisher Scientific) and transferred using a nitrocellulose membrane.

Statistical Analysis

Statistically significant differences among experimental groups were determined by one-way ANOVA or *t* test ($P < 0.05$). Data

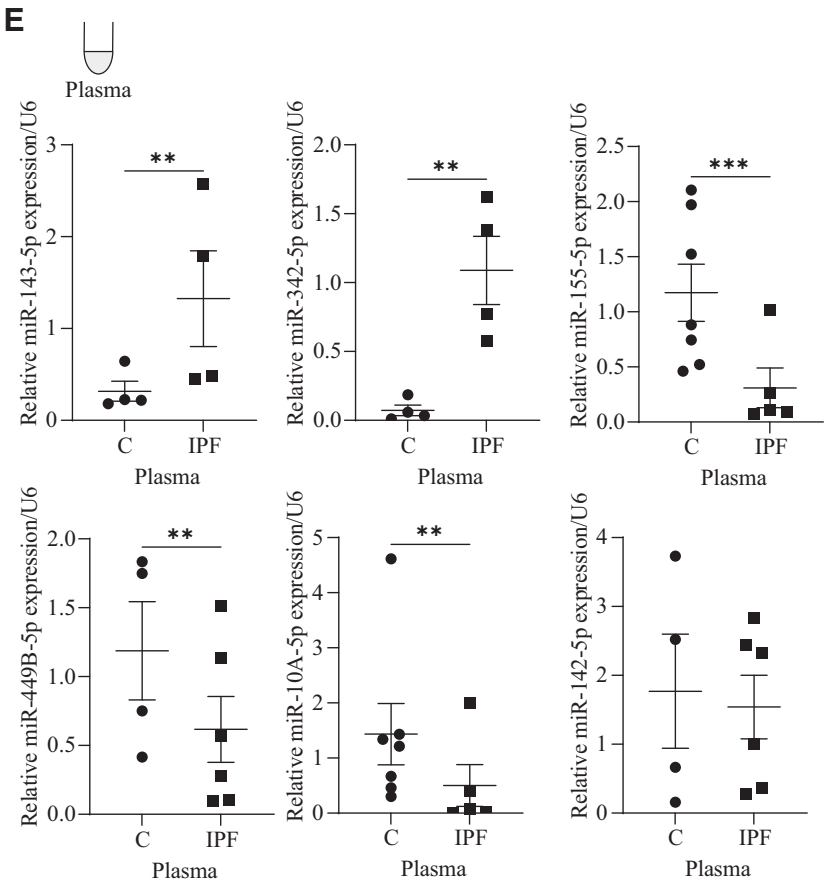

Figure 1. (*Continued*).

are shown as mean ± SEM from at least three independent experiments.

Results

Altered miRNA Expression in Plasma-Derived Exosomes in Patients with IPF

The demographic and clinical characteristics of the subjects are shown in Tables 1 and E1. The size and purity of exosomes were confirmed using NanoSight, which indicated their typical distribution (Figures 1A and 1B). The identity of the recovered vesicles as exosomes was further confirmed through the enrichment of exosomal markers CD63 and CD81 by Western blotting (Figure 1C). In addition, the absence of cytochrome c confirmed the purity of the exosome preparation. We found an increased expression of miR-143-5p, miR-342a-5p, miR-155-5p, miR-449B-5p, miR-10A-5p, and miR-142-5p in exosomes obtained from the plasma of naive patients with IPF compared with control subjects by RT-PCR (Figure 1D). Our results also indicate higher miR-143-5p and miR-342-5p expression in plasma in patients with IPF compared with control subjects (Figure 1E). miR-155-5p, miR-449B-5p, and miR-10A-5p levels were decreased in IPF. The differential expression of miRNAs in plasma-derived exosomes and whole plasma may be explained by the stability of exosomes leading to miRNA preservation compared with free circulating miRNAs. Together, our data indicate a potential role of miR-143-5p and miR-342-5p in IPF pathophysiology.

Upregulated miR-143-5p and miR-342-5p Expression in ATII Cells in IPF

Histopathological analysis of lung tissue by hematoxylin and eosin staining and Masson's trichrome staining of collagen showed severe pulmonary damage and high collagen deposition in patients with IPF compared with control subjects (Figures E1A and E1B). Our analysis revealed increased miR-143-5p and miR-342-5p expression in exosomes obtained from IPF lung tissue (Figure 2A). The levels of miR-155-5p, miR-449B-5p, and miR-10A-5p were decreased in exosomes obtained from patients with IPF compared with control subjects. Interestingly, we found an increase in the expression of all analyzed miRNAs in lung tissue from patients with IPF compared with control subjects (Figure 2B).

We detected SP-C expression in lung tissue–derived exosomes (Figure 2C), which suggests the presence of vesicles originated from ATII cells. Interestingly, we observed upregulation of miR-143-5p, miR-342-5p, miR-449B-5p, miR-10A-5p, and miR-142-5p in ATII cells in patients with IPF compared with control subjects (Figure 2D). It is worth noting that miR-143-5p and miR-342-5p expression was consistently increased in IPF in all analyzed samples: plasma, plasma-derived exosomes, lung tissue, lung tissue–derived exosomes, and ATII cells. Freshly isolated ATII cells were also analyzed using transmission electron microscopy, and we observed extracellular vesicles with the

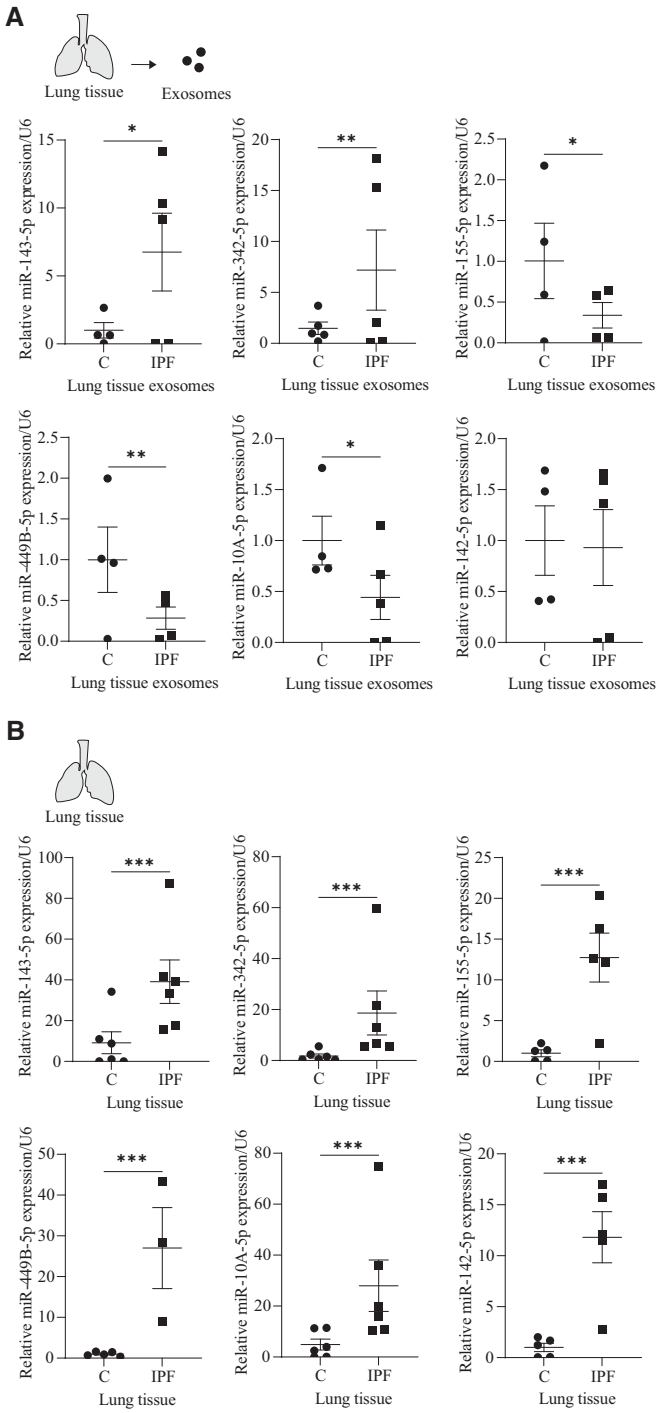

Figure 2. miRNA expression in lung tissue, alveolar type II (ATII) cells, and exosomes obtained from control subjects and patients with IPF. Samples were obtained from control organ donors and naive patients with IPF. (*A*) miRNA levels analyzed in lung tissue–derived exosomes using RT-PCR. (*B*) miRNA expression in lung tissue by RT-PCR. (*C*) Representative Western blotting image of SP-C expression in lung tissue–derived exosomes. (*D*) miRNA levels in ATII cells using RT-PCR. (*E*) ATII cell image by transmission electron microscopy (left image; scale bar, 5 μm). Vesicles are shown by black arrows (right image; scale bar, 0.2 μm). ($N = 3$–6 lungs per group. $^{*}P < 0.05$, $^{**}P < 0.01$, and $^{***}P < 0.001$.) Data are shown as means ± SEM.

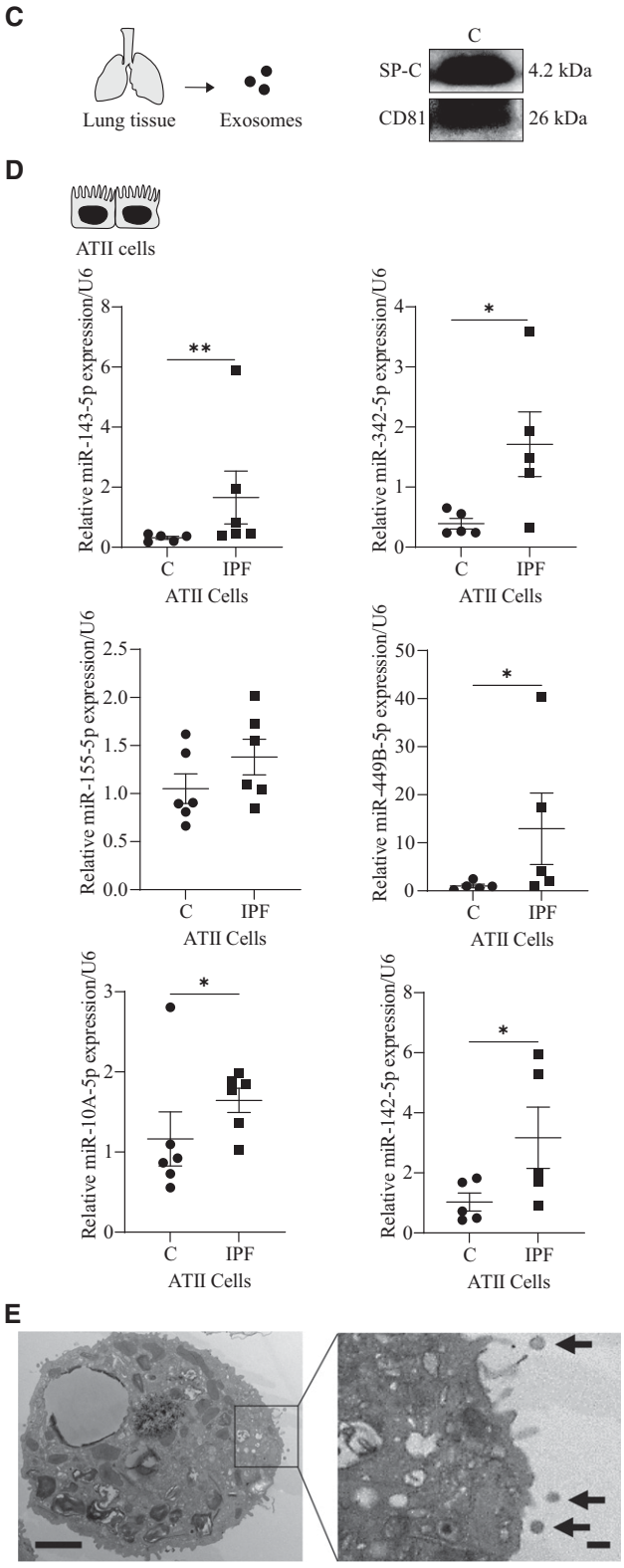

Figure 2. (*Continued*).

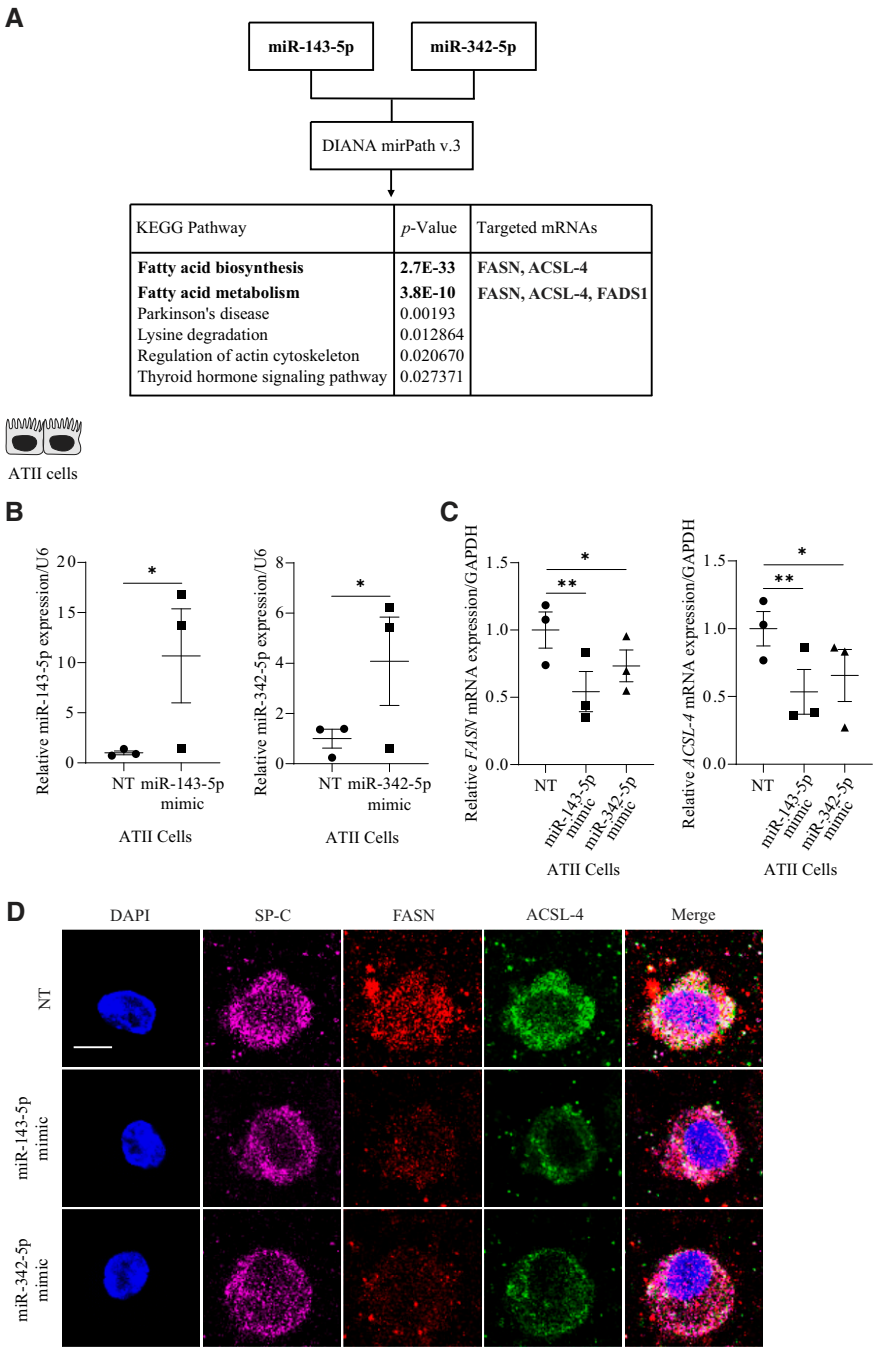

Figure 3. Overexpression of miR-143-5p and miR-342-5p mimics in ATII cells. (*A*) *In silico* analysis using DIANA miRPath v.3 shows miR-143-5p and miR-342-5p targets. (*B*) ATII cells were isolated from control organ donors. Cultured cells were transfected with miR-143-5p and miR-342-5p mimics, and their overexpression was confirmed by RT-PCR. (*C*) *FASN* (fatty acid synthase) and *ACSL-4* (acyl-CoA-synthetase long-chain family member 4) mRNA levels in ATII cells with miR-143-5p and miR-342-5p mimic overexpression were determined by RT-PCR. (*D*) ATII cells were stained using SP-C (magenta), FASN (red), and ACSL-4 (green) antibodies and DAPI (blue) by immunofluorescence using confocal microscopy. Scale bars, 5 μm. (*E*) Quantification of fluorescence intensity is also shown. (*F*) *FASN* and *ACSL-4* mRNA levels in lung tissue were evaluated by RT-PCR. (*G*) Representative images of FASN and ACSL-4 protein expression in lung tissue by Western blotting. (*H*) Quantification of protein expression normalized to GAPDH. (*I*) *FASN* and *ACSL-4* mRNA levels in ATII cells by RT-PCR. (*J*) FASN and ACSL-4 protein expression in ATII cells by Western blotting. (*K*) Quantification of protein expression is shown. (*L*) *FASN* mRNA levels in ATII cells treated with TVB-3664 were detected by RT-PCR. (*M*) miR-143-5p and miR-342-5p expression in ATII cells treated with TVB-3664, detected by RT-PCR. (*N*) ATII cells were stained using SP-C (magenta), FASN (red) antibodies, and DAPI (blue) by immunofluorescence using confocal microscopy. Scale bars, 5 μm. (*O*) Quantification of FASN and SP-C fluorescence intensity. (*P*) *P53* and *P21* mRNA levels in ATII cells by RT-PCR. ($N = 3$–8 lungs per group. $^{*}P < 0.05$, $^{**}P < 0.01$, and $^{***}P < 0.001$.) Data are shown as means ± SEM. NT = non-target.

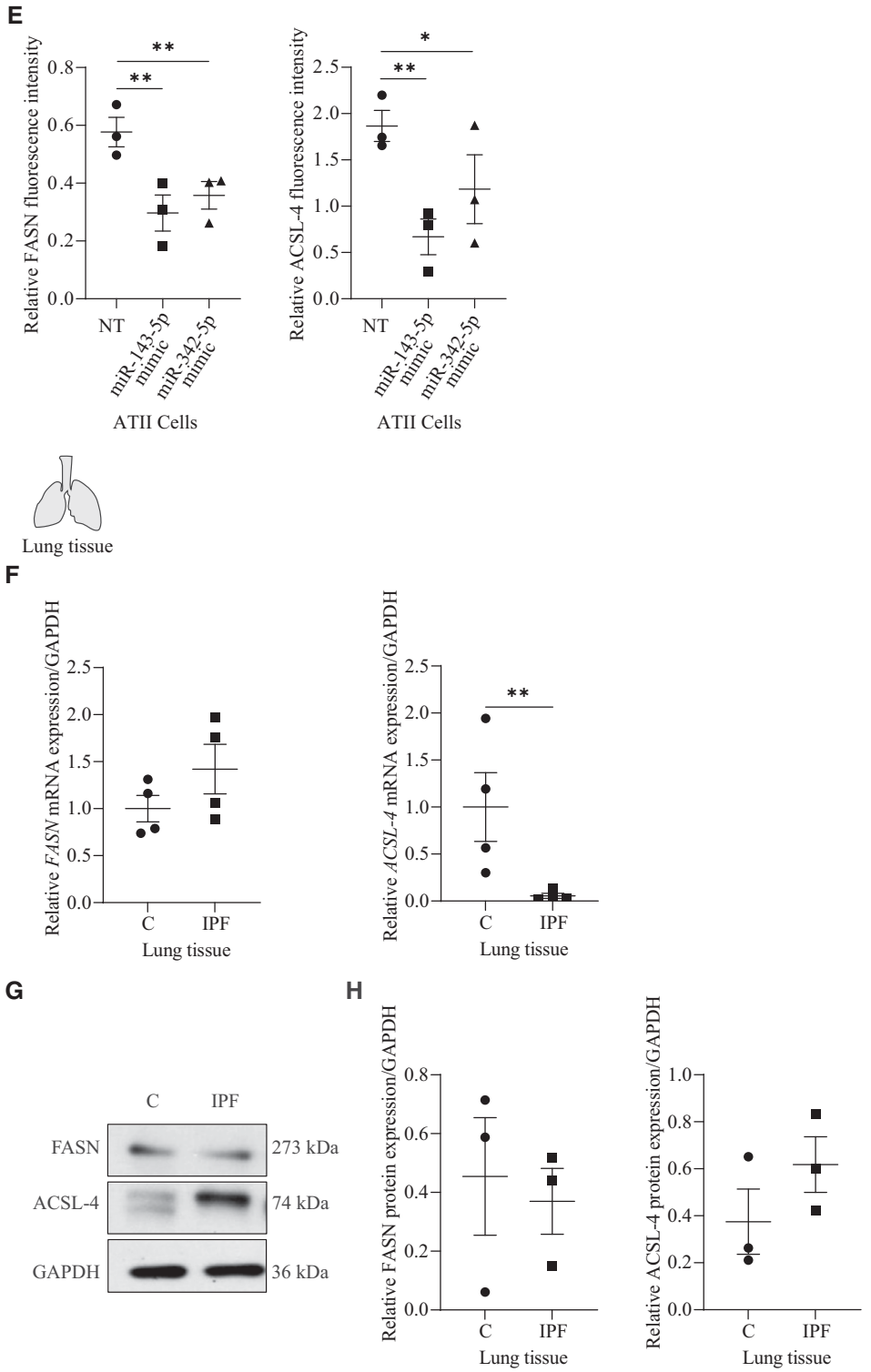

Figure 3. (*Continued*).

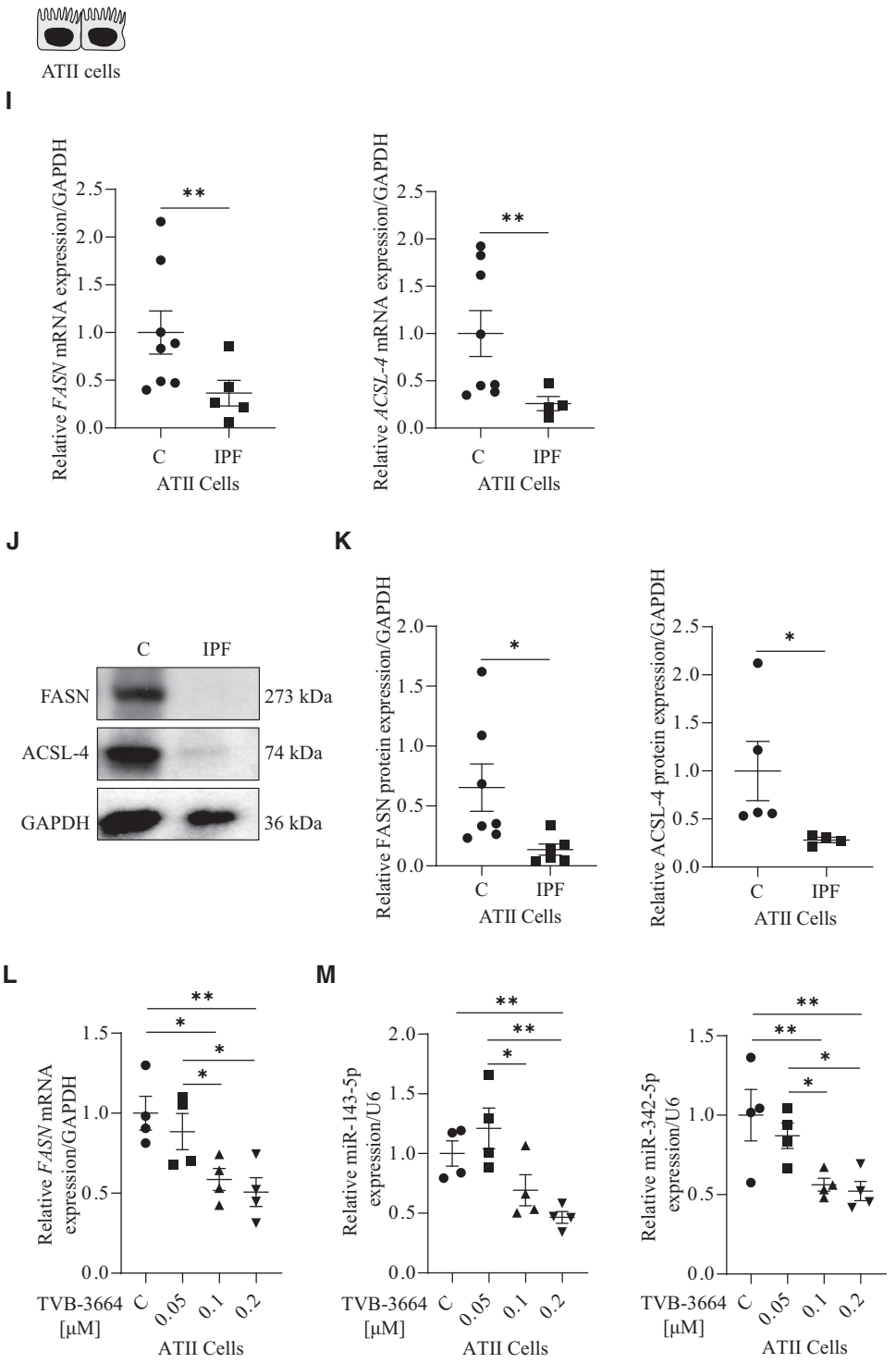

Figure 3. (*Continued*).

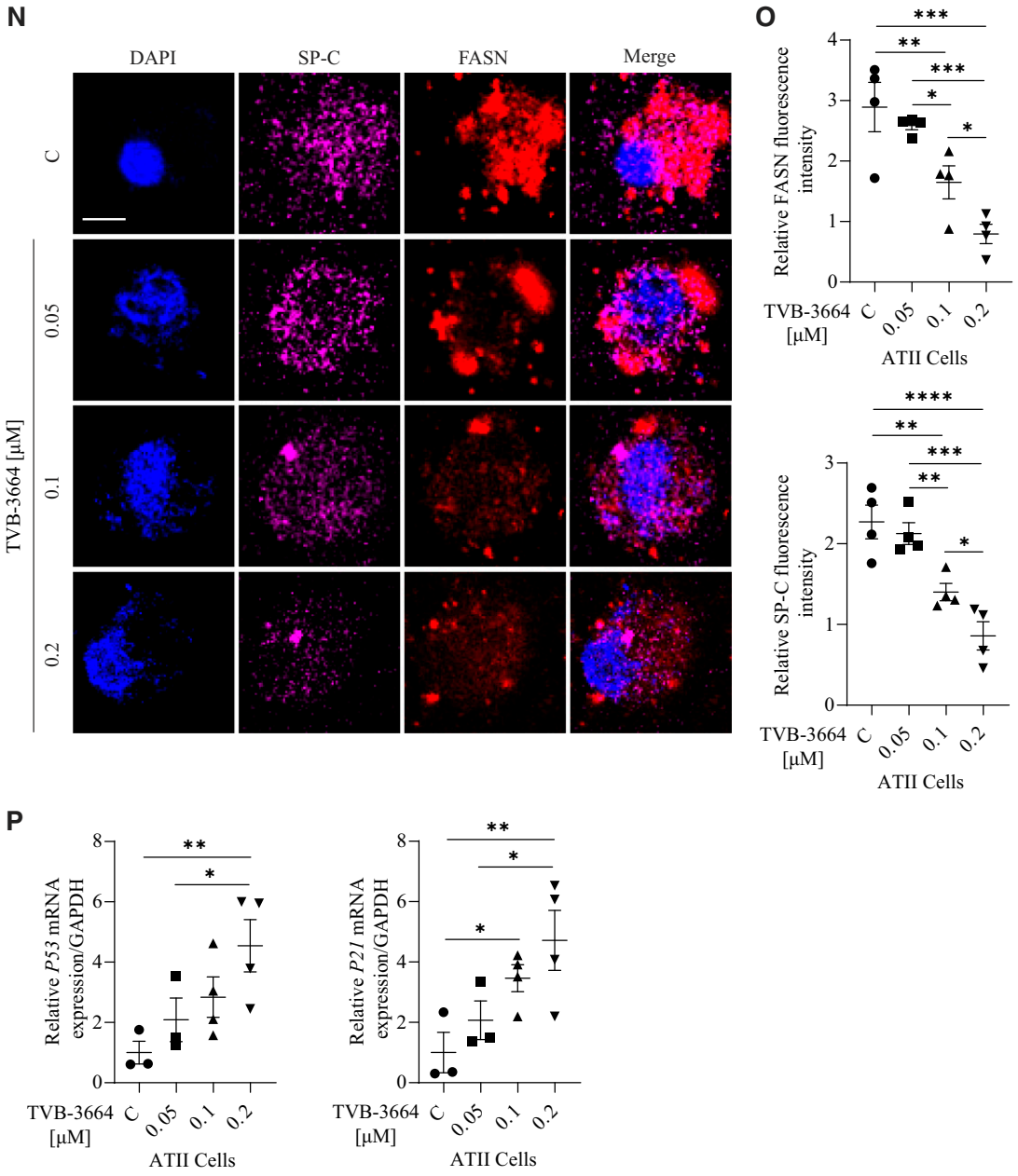

Figure 3. (*Continued*).

size of exosomes (Figure 2E). Our results suggest that ATII cell–derived exosomes may contribute to the high expression of miR-143-5p and miR-342-5p in IPF.

Because exosome molecular cargoes are highly heterogeneous and cell-type dependent, we also analyzed miR-143-5p and miR-342-5p levels in exosomes obtained from lung fibroblasts. Their expression was higher in patients with IPF than in control subjects (Figure E2A). Also, an increased miR-342-5p level was found in alveolar macrophages isolated from patients with IPF (Figure E2B). We did not detect significant differences in miR-143-5p expression between these groups.

Decreased FASN and ACSL-4 Expression in ATII Cells in IPF

We used *in silico* analysis (DIANA-miRPath) and detected that miR-143-5p and miR-342-5p are implicated in fatty acid biosynthesis and metabolism (Figure 3A). To determine whether miR-143-5p and miR-342-5p directly target FASN and ACSL-4, we overexpressed them in cultured ATII cells obtained from control organ donors using miRNA mimics. Overexpression of miR-143-5p and miR-342-5p was confirmed by RT-PCR (Figure 3B). We also analyzed *FASN* and *ACSL-4* mRNA levels and found their significant decrease after cell transfection with miR-143-5p and miR-342-5p mimics (Figure 3C). This transfection also downregulated FASN and ACSL-4 protein levels as detected by immunofluorescence

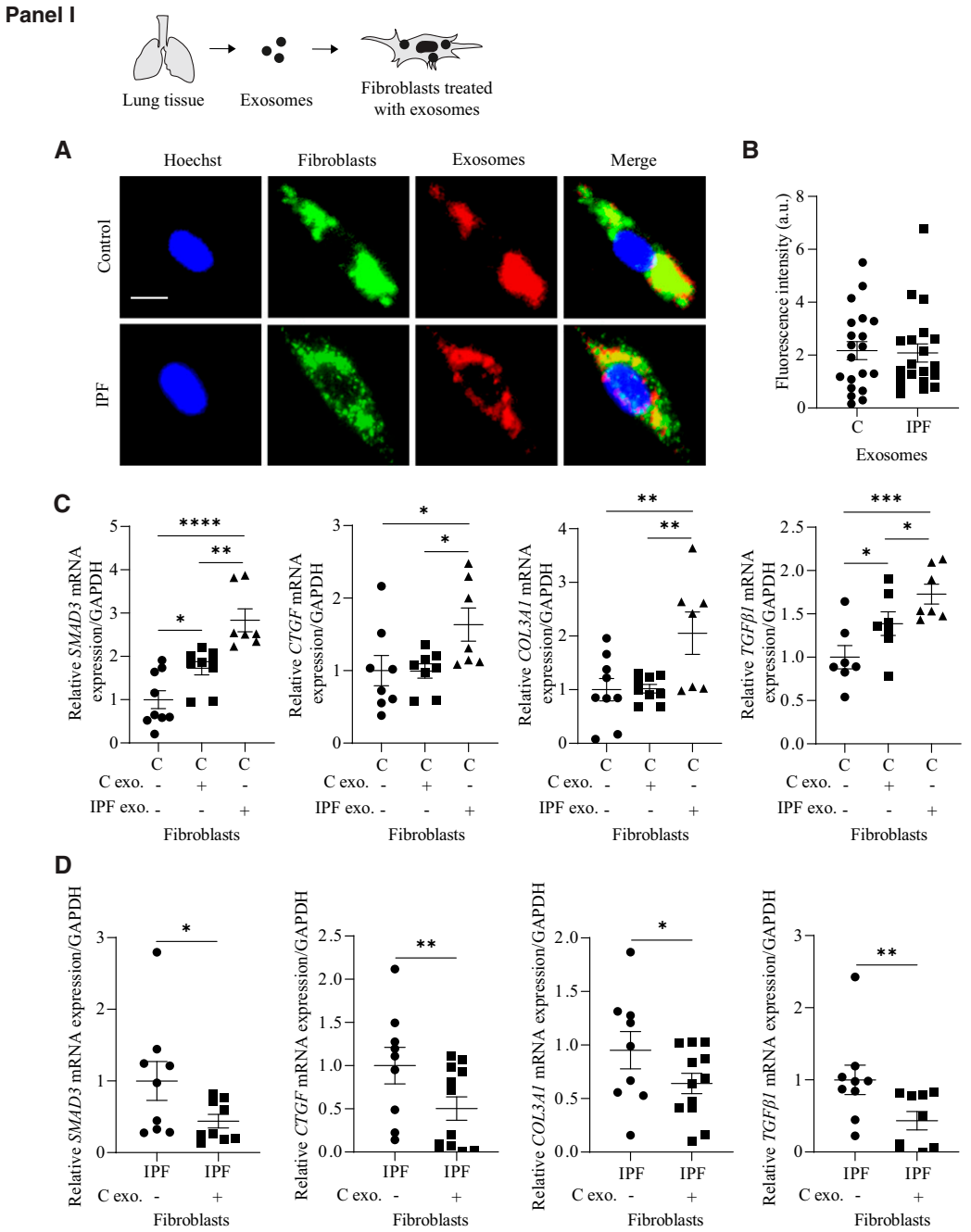

Figure 4. IPF-derived exosomes enhance profibrotic response in control fibroblasts and decrease FASN and ACSL-4 expression in control ATII cells. Panel I: Cultured lung fibroblasts and ATII cells isolated from control organ donors were treated with lung tissue–derived exosomes obtained from naive patients with IPF. (*A*) Exosomes stained with PKH26 dye (red) were internalized by fibroblasts labeled with PKH67 (green) and Hoechst 33342 (blue; scale bar, 10 μm). (*B*) Quantification of exosome internalization by fibroblasts is shown. (*C*) *SMAD3*, *CTGF*, *COL3A1*, and *TGFβ1* mRNA levels in fibroblasts treated with exosomes by RT-PCR. (*D*) Fibroblasts obtained from IPF were treated with lung tissue–derived exosomes isolated from control organ donors. *SMAD3*, *CTGF*, *COL3A1*, and *TGFβ1* mRNA levels were detected by RT-PCR. Panel II: Overexpression of miR-143-5p and miR-342-5p mimics in cultured lung fibroblasts. (*A*) miR-143-5p and miR-342-5p mimic overexpression was confirmed by RT-PCR. (*B*) *FASN* and *ACSL-4* mRNA expression in fibroblasts detected by RT-PCR. (*C*) *SMAD3*, *CTGF*, *COL3A1*, and *TGFβ1* mRNA levels by RT-PCR. Panel III: The impact of exosomes on cultured ATII cells isolated from control organ donors. (*A*) Exosomes stained with PKH26 dye (red) were internalized by ATII cells labeled by PKH67 dye (green) and Hoechst 33342 (blue; scale bar, 10 μm). (*B*) Quantification of exosome internalization by ATII cells is shown. (*C*) miR-143-5p and miR-342-5p levels in ATII cells treated with exosomes obtained from patients with IPF. (*D*) *FASN*, *ACSL-4*, and *SP-C* mRNA levels in ATII cells treated with exosomes by RT-PCR. ($N = 3$–9 lungs per group; $^{*}P < 0.05$, $^{**}P < 0.01$, $^{***}P < 0.001$, and $^{****}P < 0.0001$.) Data are shown as means ± SEM. Exo = exosomes.

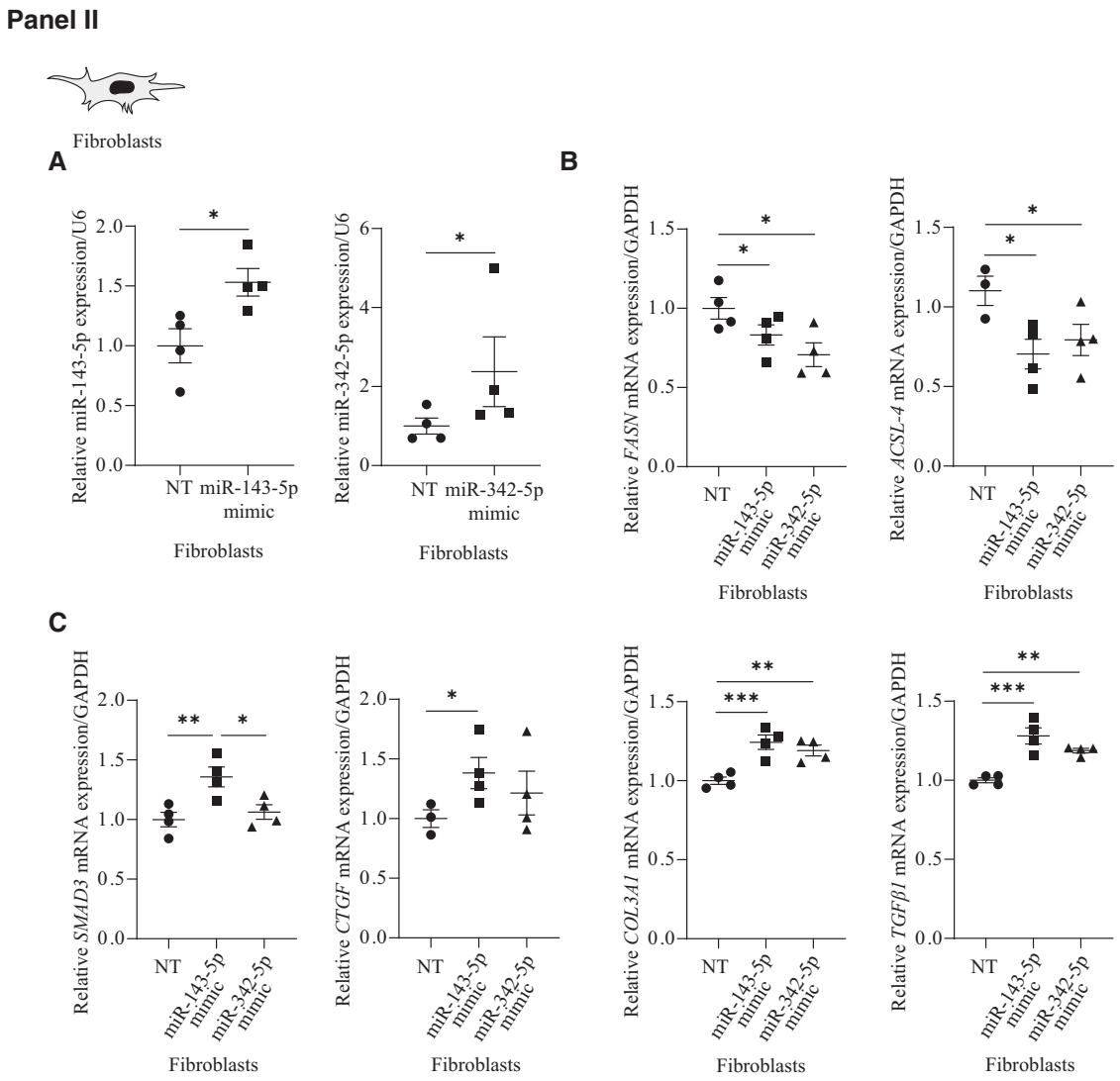

Figure 4. (*Continued*).

(Figures 3D and 3E). Also, A549 cells were transfected with pcDNA-3.1-miR-143-5p and pcDNA-3.1-miR-342-5p, and their overexpression was confirmed in A549 cells (Figures E3A–E3H). This lowered *FASN* and *ACSL-4* mRNA and protein expression. Together, our results suggest that miR143-5p and miR-342-5p can serve as new miRNA targets of key genes of *de novo* fatty acid biosynthesis, FASN, and ACSL-4. Overexpression of miR-143-5p and miR-342-5p significantly reduced the migration rate of A549 cells after 48 hours compared with controls using a scratch assay (Figures E3I and E3J). The efficiency of cell transfection is shown in Figure E4. Our results suggest their contribution to the delayed repair of lung epithelial cells after injury.

ACSL-4 mRNA levels were decreased in lung tissue in patients with IPF compared with control subjects (Figure 3F). We did not detect any differences between FASN and ACSL-4 protein expression in lung tissue from patients with IPF compared with control subjects by Western blotting (Figures 3G and 3H). Interestingly, we observed a significant decrease in *FASN* and *ACSL-4* mRNA levels in ATII cells in IPF (Figure 3I). We found the same correlation for FASN and ACSL-4 protein expression (Figures 3J and 3K). Moreover, we cultured ATII cells to examine whether inhibition of FASN expression with TVB-3664, which is the novel fatty acid synthase inhibitor (27) affects miR-143-5p and miR-342-5p levels. We found that 0.1 μM and 0.2 μM TVB-3664 significantly reduced *FASN* mRNA expression (Figure 3L) and the levels of miR-143-5p and miR-342-5p (Figure 3M). These data suggest that in ATII cells in IPF, miR-143-5p and 342-5p inhibit FASN expression, which promotes these miR expressions, forming a feedback loop. We also confirmed the decrease of FASN, SP-C, and PGC1α levels by TVB-3664 treatment (Figures 3N, 3O, and E5). Furthermore, we found that FASN inhibition increased the expression of senescence markers such as *P53* and *P21* as detected by RT-PCR (Figure 3P). Together, our data suggest that miR-143-5p and miR-342-5p may contribute to ATII cell dysfunction in IPF through the dysregulation of *de novo* fatty acid biosynthesis and induce cell senescence.

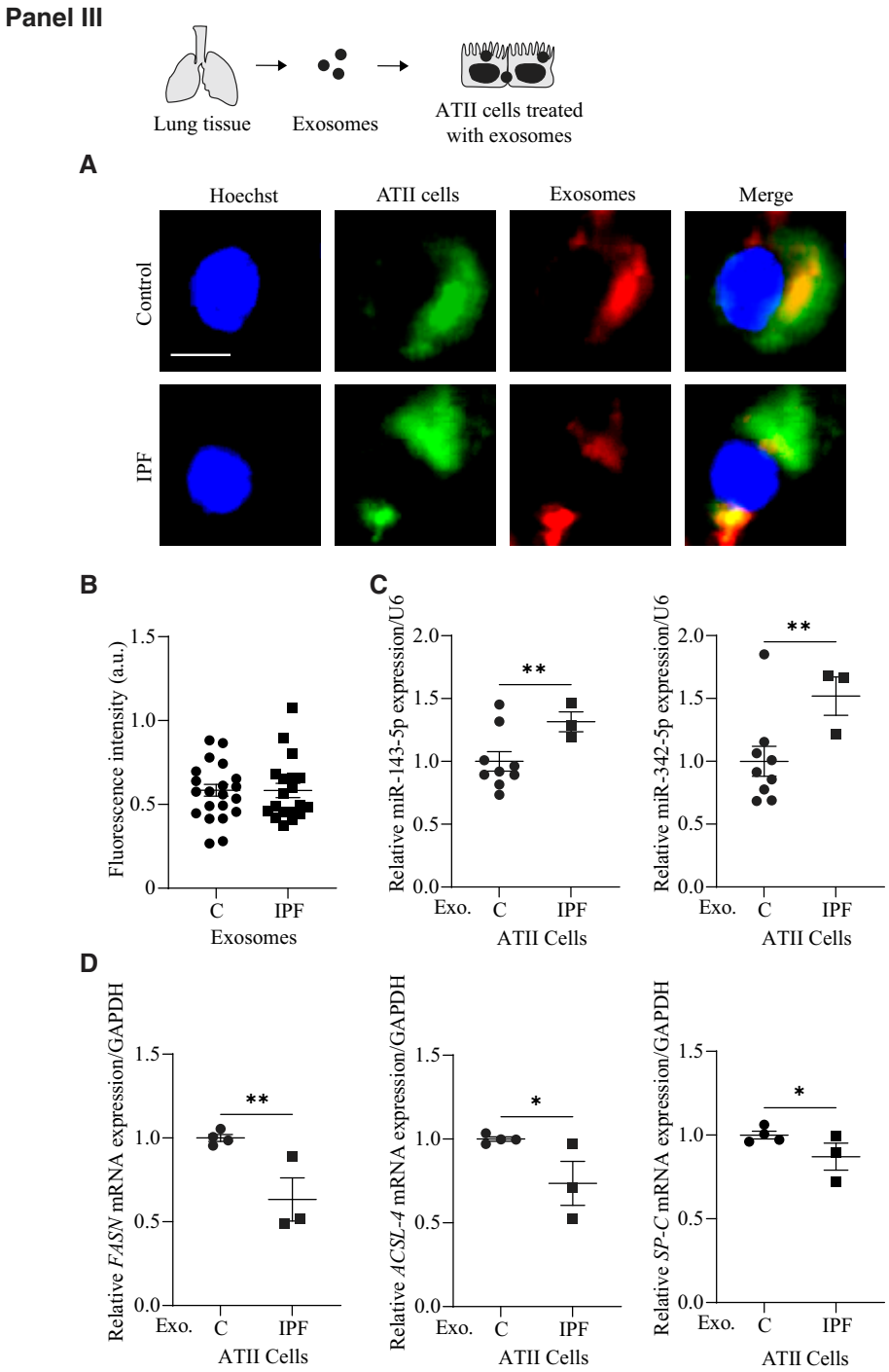

Figure 4. (*Continued*).

IPF-derived Exosomes Enhance Profibrotic Response in Control Lung Fibroblasts and Decrease FASN and ACSL-4 Expression in Control ATII Cells

We wanted to determine the effect of lung tissue–derived exosomes obtained from patients with IPF on fibroblasts isolated from control organ donors. Exosomes were labeled with PHK26 dye and incubated for 24 hours with cultured fibroblasts stained with PKH67 reagent. Their internalization by fibroblasts was detected using fluorescence microscopy (Figure 4, Panel I, A). There was no difference in the exosome uptake by fibroblasts obtained from control subjects and patients with IPF (Figure 4, Panel I, B). To investigate whether IPF exosome uptake by control fibroblasts modulates cellular responses, we assessed *SMAD3*, *CTGF*, *COL3A1*, and *TGFβ1* levels by RT-PCR. Cell treatment with exosomes obtained from IPF lung tissue significantly increased mRNA expression levels of these profibrotic genes

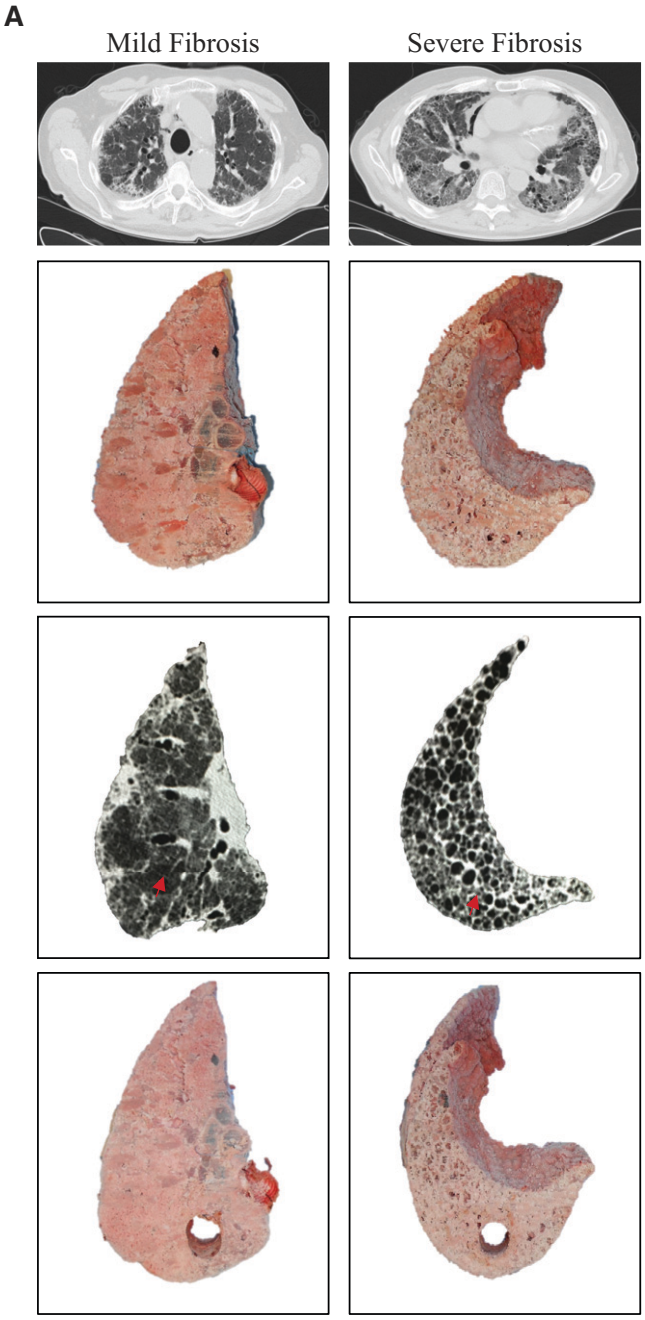

Figure 5. Increased miR-143-5p and miR-342-5p levels in severe fibrosis. (*A*) Representative computed tomography scan of IPF lung with mild and severe fibrosis in the same patient. (*B*) miR-143-5p and miR-342-5p levels in tissue obtained from mild and severe fibrosis areas by RT-PCR. (*C*) miR-143-5p and miR-342-5p expression in lung tissue–derived exosomes isolated from mild and severe fibrosis areas. (*D*) Fibroblasts obtained from control organ donors were cultured. *SMAD3*, *CTGF*, *COL3A1*, and *TGFβ1* mRNA levels in fibroblasts treated with lung tissue–derived exosomes isolated from mild and severe fibrosis areas ($N = 3$–4 lungs; $^{*}P < 0.05$ and $^{**}P < 0.01$.) Data are shown as means ± SEM.

(Figure 4, Panel I, C). Our data highlight the profibrotic features of IPF exosomes via activating the TGFβ signaling pathway in control fibroblasts. Next, we wanted to determine the impact of lung tissue–derived exosomes obtained from control organ donors on fibroblasts isolated from IPF. Interestingly, treatment with exosomes for 24 hours decreased *SMAD3*, *CTGF*, *COL3A1*, and *TGFβ1* expression in IPF fibroblasts compared with untreated cells (Figure 4, Panel I, D).

Cultured fibroblasts isolated from control organ donors were treated with exosomes obtained from patients with IPF,

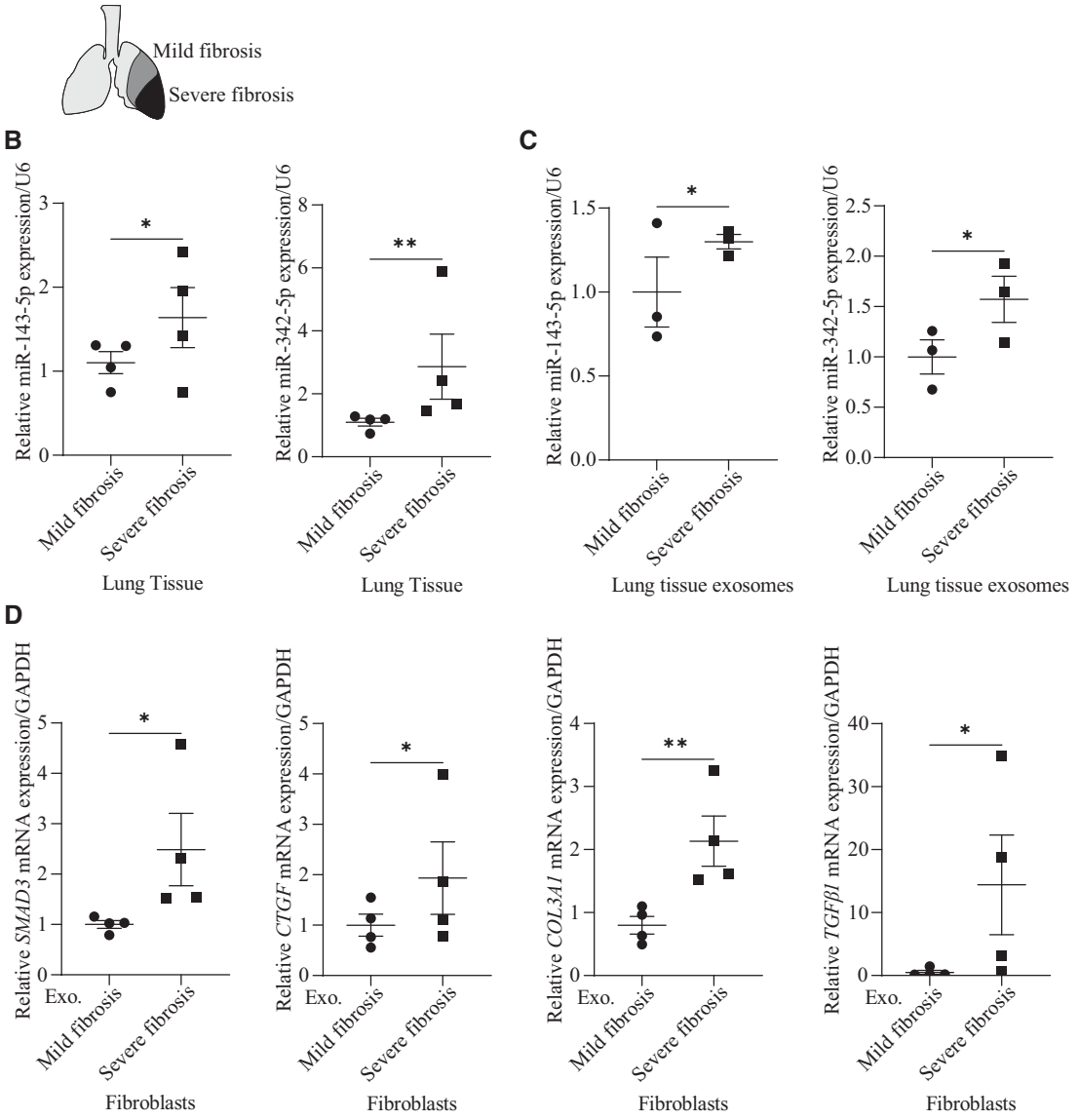

Figure 5. (*Continued*).

which increased miR-143-5p and miR-342-5p levels (Figure E6, Panel I, A). Moreover, we found decreased *FASN* and *ACSL-4* mRNA expression (Figure E6, Panel I, B). These results suggest that increased miR-143-5p and miR-342-5p expression in fibroblasts may also affect *FASN* and *ACSL-4* levels. We did not detect any differences between FASN and ACSL-4 protein expression between these two groups by Western blotting (Figure E6, Panel I, C and D). Next, we examined whether treatment with exosomes obtained from IPF affected other fatty acid synthesis pathway enzymes, such as ACACA (Acetyl-coA-carb-α) and ACLY (ATP-citrate-lyase). However, there was no significant difference between *ACACA* and *ACLY* mRNA levels in fibroblasts treated with exosomes obtained from patients with IPF compared with control subjects (Figure E6, Panel I, E). These data indicate that IPF-derived exosomes may specifically affect FASN and ACSL-4. We further investigated the impact of IPF-derived exosomes on fibroblast senescence, and we did not detect changes in *P16*, *P21*, or *P53* expression by RT-PCR (Figure E6, Panel I, F). This suggests that exosomes obtained from patients with IPF did not induce senescence in fibroblasts.

Higher miR-143-5p and miR-342-5p levels and decreased *FASN* and *ACSL-4* mRNA expression were found in fibroblasts obtained from patients with IPF compared with control subjects (Figures E7A and E7B). ACSL-4 protein expression was downregulated in IPF fibroblasts by Western blotting (Figures E7C and E7D). Next, we examined the levels of profibrotic markers in fibroblasts obtained from IPF using RT-PCR. Increased *SMAD3*, *CTGF*, *COL3A1*, and *TGFβ1* mRNA expression was found in IPF

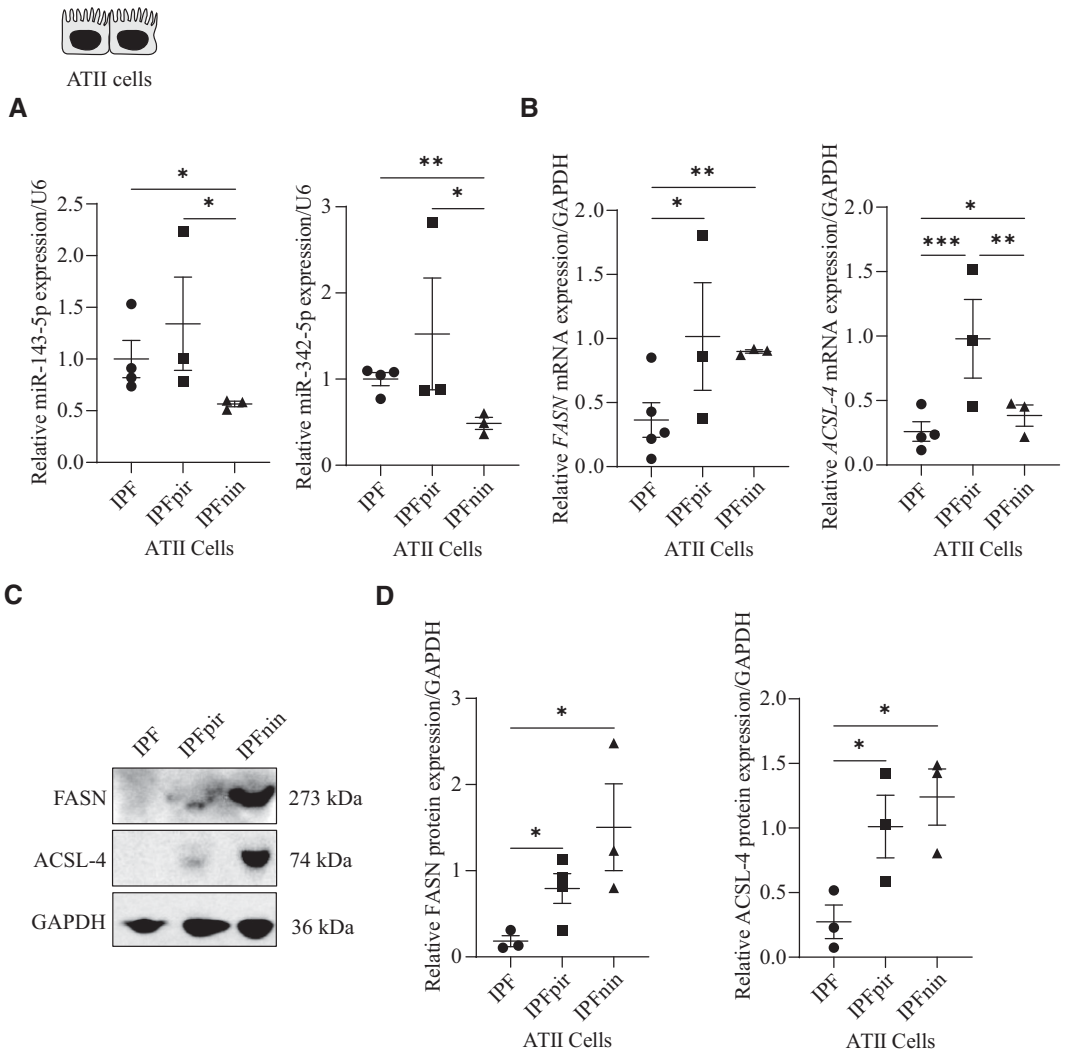

Figure 6. Pirfenidone and nintedanib increased FASN and ACSL-4 expression in ATII cells in patients with IPF. Cultured ATII cells and fibroblasts isolated from control organ donors were treated with lung tissue–derived exosomes obtained from naive patients with IPF and patients with IPF treated with pirfenidone (pir) or nintedanib (nin). (*A*) miR-143-5p and miR-342-5p expression in ATII cells isolated from patients with IPF by RT-PCR. (*B*) *FASN* and *ACSL-4* mRNA levels in ATII cells isolated from IPF using RT-PCR. (*C*) Representative Western blotting images of FASN and ACSL-4 expression in ATII cells. (*D*) Quantification of protein expression is also shown. (*E*) Cultured ATII cells were treated with lung tissue–derived exosomes obtained from naive patients with IPF and medicated patients with IPF. Cells were stained using SP-C (magenta), FASN (red), and ACSL-4 (green) antibodies and DAPI (blue) by immunofluorescence using confocal microscopy. (*F*) Quantification of their fluorescence intensity is also shown. (*G*) *SP-C*, *FASN*, and *ACSL-4* mRNA levels by RT-PCR in ATII cells treated with exosomes obtained from naive patients with IPF and patients with IPF treated with pirfenidone or nintedanib. (*H*) *SMAD3*, *CTGF*, *COL3A1*, and *TGFβ1* mRNA levels by RT-PCR in fibroblasts treated with lung tissue–derived exosomes obtained from naive patients with IPF and medicated patients with IPF. Cultured ATII cells isolated from organ donors were treated with exosomes obtained from the lung tissue of naive patients with IPF or patients with IPF medicated with pirfenidone or nintedanib. (*I*) *P53*, *P16*, *P21*, and *IL-6* mRNA levels in ATII cells by RT-PCR. (*J*) ATII cells were stained using SP-C (magenta), p-P53 (red), and P53 (green) antibodies and DAPI (blue) by immunofluorescence using confocal microscopy. (*K*) Quantification of p-P53/P53 is also shown. (*L*) ATII cells were stained using SP-C (magenta), P16 (red), and P21 (green) antibodies and DAPI (blue) by immunofluorescence using confocal microscopy. (*M*) Quantification of their fluorescence intensity is also shown. (*N*) Representative images of SA-β-Gal staining in ATII cells. (*O*) The quantification of SA-β-Gal–positive ATII cells ($N = 3$–9 lungs per group. Scale bars, 5 μm. $^{*}P < 0.05$, $^{**}P < 0.01$, $^{***}P < 0.001$, and $^{****}P < 0.0001$.) Data are shown as means ± SEM.

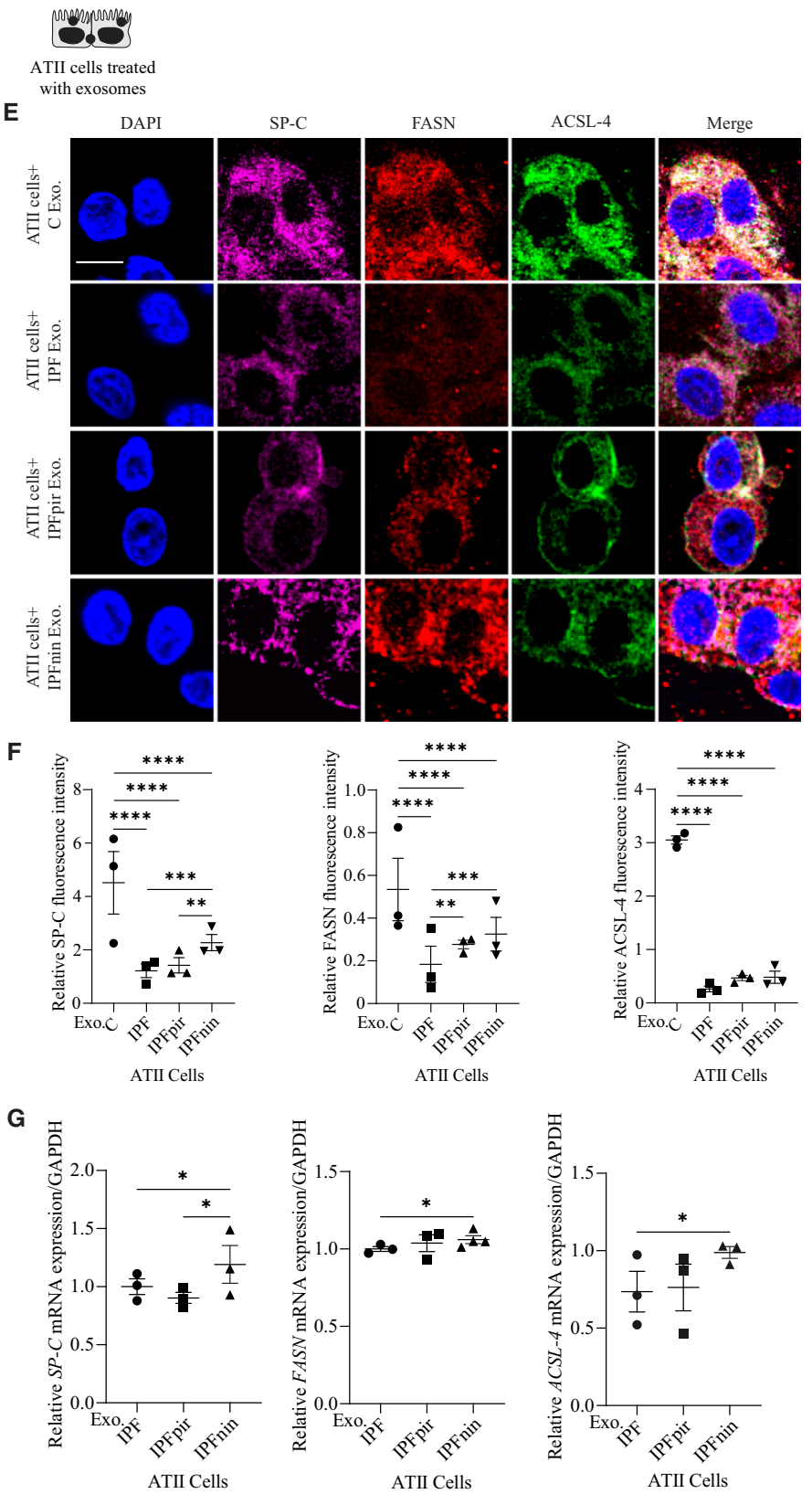

Figure 6. (*Continued*).

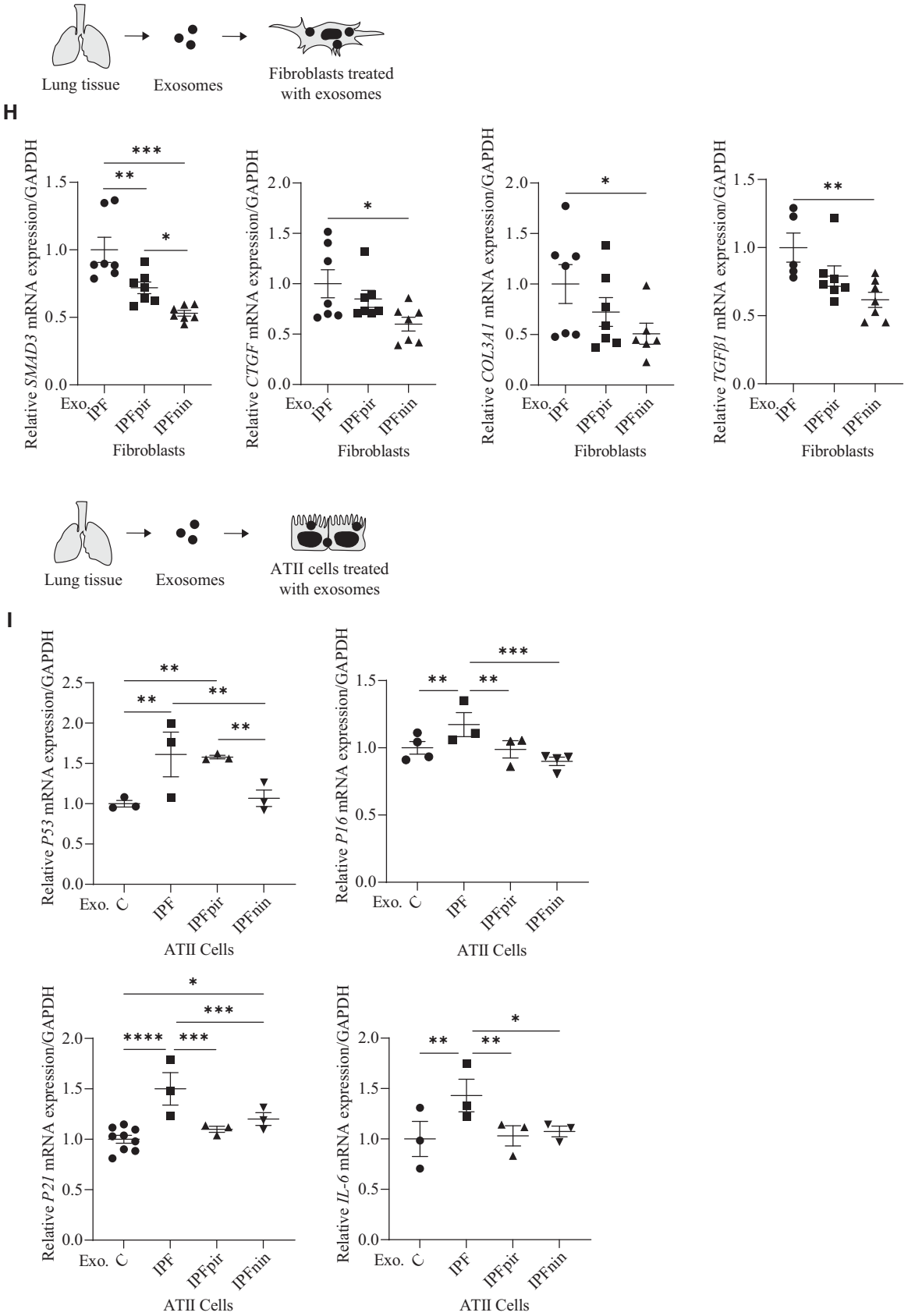

Figure 6. (*Continued*).

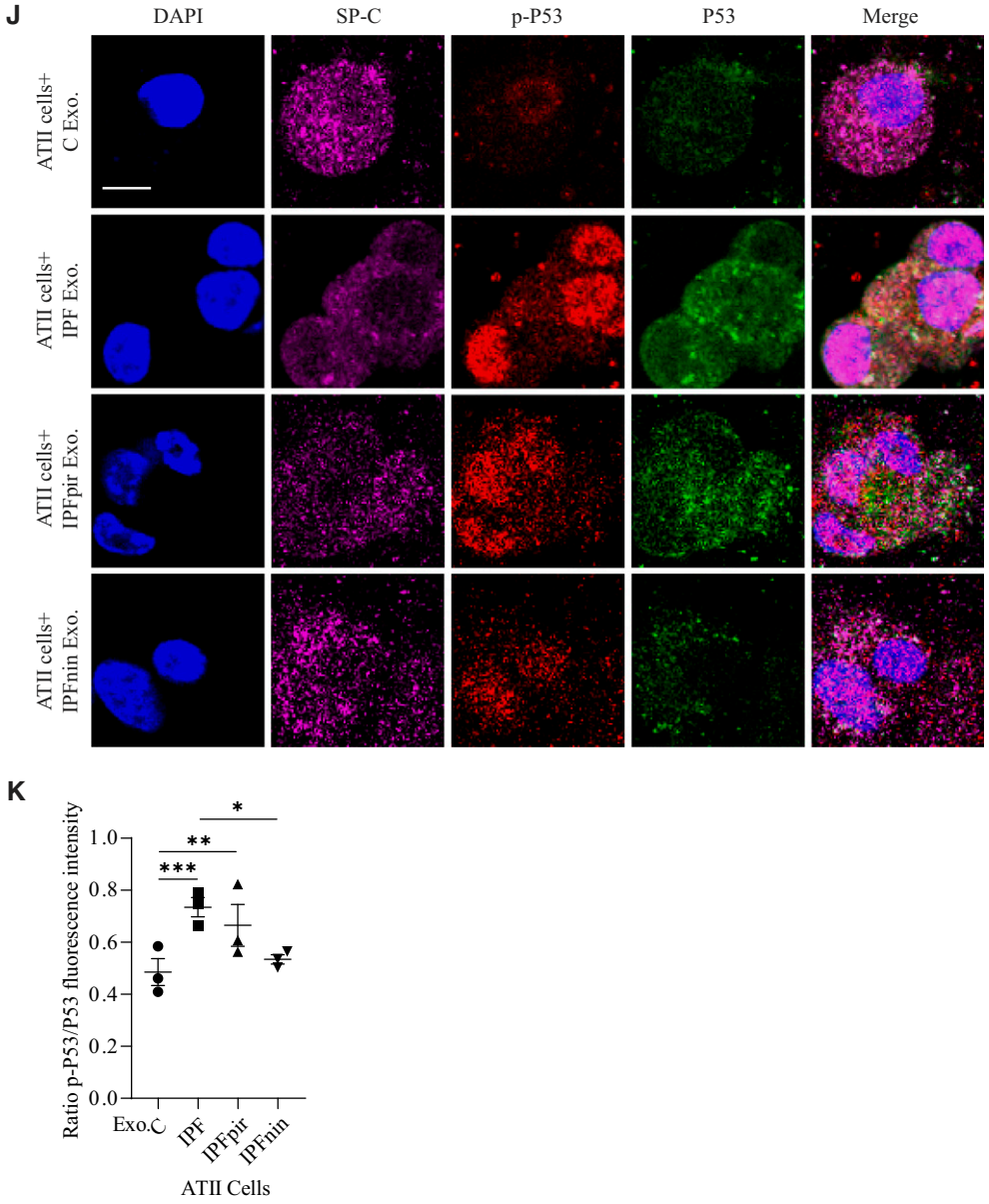

Figure 6. (*Continued*).

fibroblasts compared with controls (Figure E7E).

To determine whether the profibrotic response in fibroblasts is correlated with miR-143-5p and miR-342-5p levels, we overexpressed them in control cultured fibroblasts using miR mimics. Their overexpression was confirmed by RT-PCR (Figure 4, Panel II, A). We analyzed *FASN* and *ACSL-4* mRNA levels and found their decreased expressions after cell transfection with miR-143-5p and miR-342-5p mimics (Figure 4, Panel II, B). Overexpression of miR-143-5p increased *SMAD3*, *CTGF*, *COL3A1*, and *TGFβ1* levels, whereas miR-342-5p mimic upregulated *COL3A1* and *TGFβ1* expression as detected by RT-PCR (Figure 4, Panel II, C). Our data suggest that miR-143-5p and miR-342-5p may activate control fibroblasts' transition to myofibroblast.

To determine the impact of vesicles, we treated cultured ATII cells with lung tissue–derived exosomes obtained from control subjects and patients with IPF for 24 hours (Figure 4, Panel III, A). ATII cells internalized exosomes at the same rate (Figure 4, Panel III, B). Importantly, the internalization of IPF exosomes increased miR-143-5p and miR-342-5p levels in ATII cells, suggesting the transfer of their content to ATII cells (Figure 4, Panel III, C). Because we detected the enrichment of miR-143-5p and miR-342-5p in ATII cells in IPF, we also wanted to analyze their impact on cell function. Cultured ATII cells treated with IPF exosomes had significantly decreased *FASN*, *ACSL-4*, and *SP-C* mRNA expression compared with control exosomes as detected

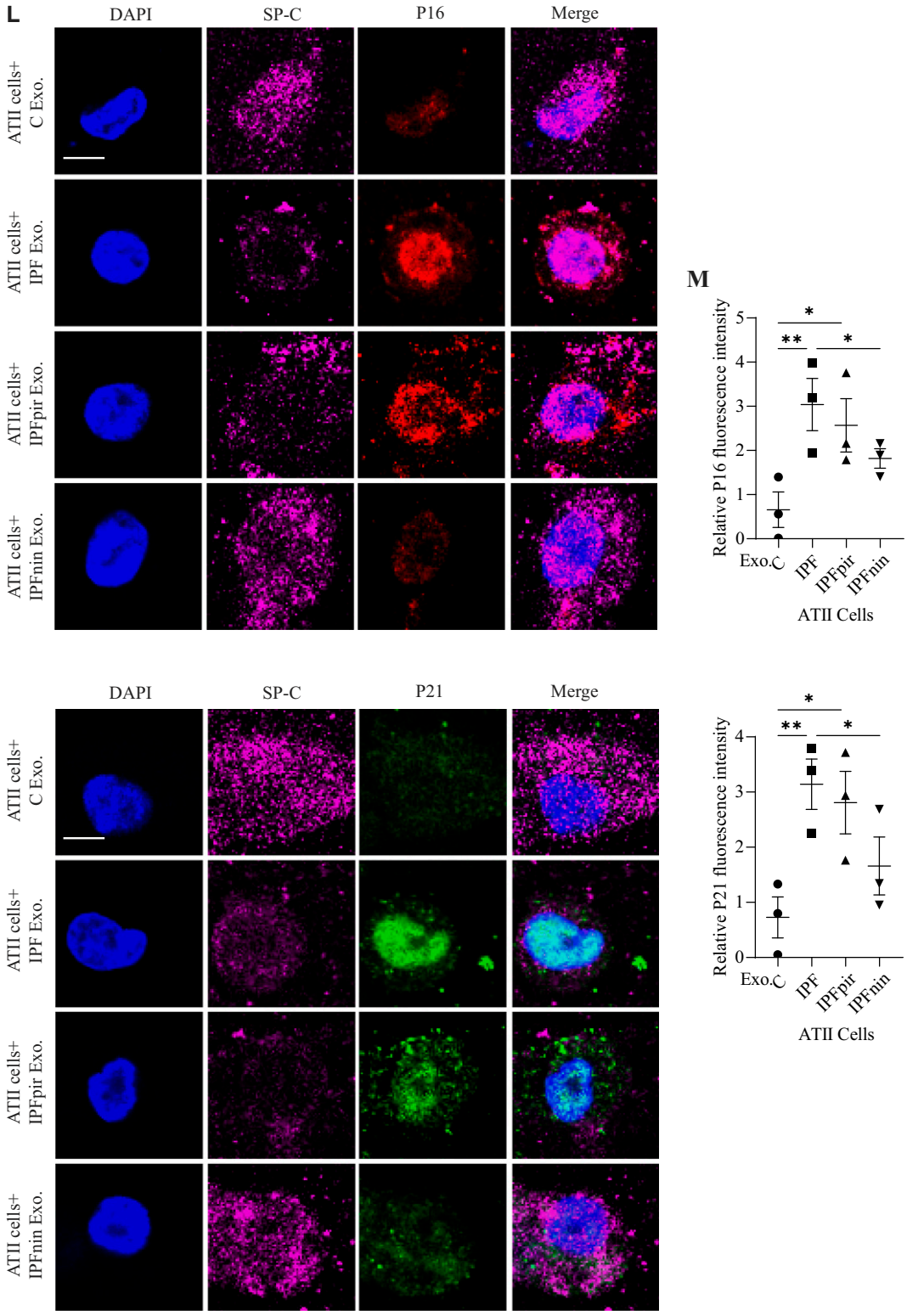

Figure 6. (*Continued*).

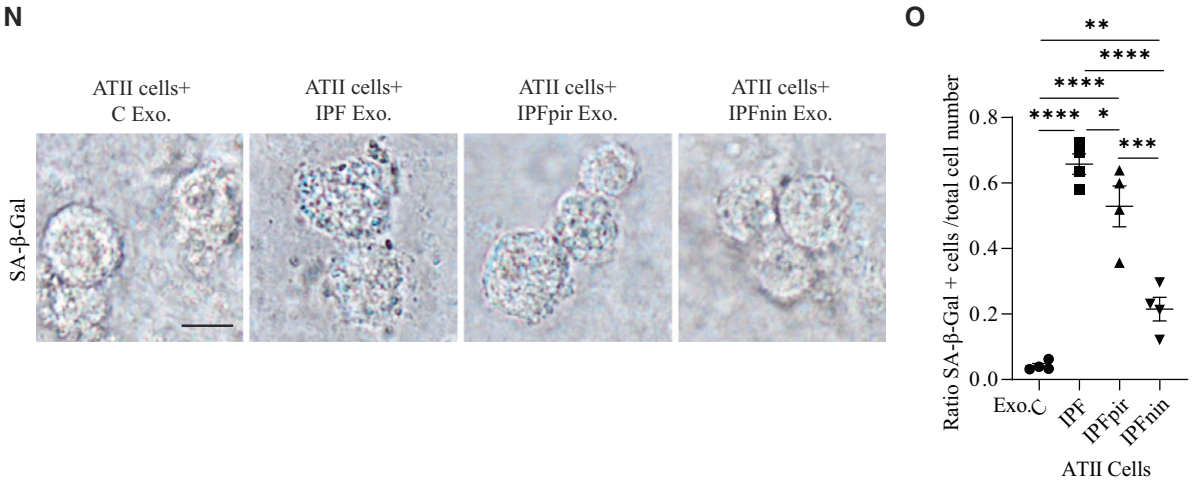

Figure 6. (*Continued*).

by RT-PCR (Figure 4, Panel III, D). Our results indicate that IPF-derived exosomes decreased *de novo* fatty acid biosynthesis in ATII cells through their internalization.

The Role of Exosomes in Human Mild and Severe Fibrosis

We used lung tissue obtained from the areas of mild and severe fibrosis of the same patient with IPF based on the computed tomography scan (Figure 5A). Interestingly, we found increased miR-143-5p and miR-342-5p levels in lung tissue in severe compared with mild fibrosis by RT-PCR (Figure 5B). Moreover, we detected an enrichment of these miRNAs in exosomes isolated from severe areas (Figure 5C). The effect of exosomes was analyzed on cultured fibroblasts isolated from control organ donors. Exosomes obtained from severe fibrosis areas significantly induced *SMAD3*, *CTGF*, *COL3A1*, and *TGFβ1* mRNA expression (Figure 5D). Our results suggest the role of miR-143-5p and miR-342-5p in IPF progression through exosome-mediated profibrotic response.

Pirfenidone and Nintedanib Upregulate FASN and ACSL-4 Expression in ATII Cells

ATII cells were isolated from naive patients with IPF and patients with IPF taking antifibrotic drugs. We found that nintedanib decreased miR-143-5p and miR-342-5p expression in ATII cells compared with naive individuals with IPF and individuals taking pirfenidone (Figure 6A). Both drugs increased *FASN* and *ACSL-4* mRNA levels in ATII cells as detected by RT-PCR (Figure 6B). Importantly, FASN and ACSL-4 levels were higher in ATII cells isolated from patients treated with pirfenidone or nintedanib compared with naive patients with IPF by Western blotting (Figures 6C and 6D). Our results suggest that antifibrotic drugs affect the fatty acid synthesis pathway in ATII cells.

To further define the impact of medication, control cultured ATII cells were treated with lung tissue–derived exosomes obtained from control subjects, naive subjects with IPF, and patients with IPF taking pirfenidone or nintedanib, followed by analysis using immunofluorescence (Figure 6E). SP-C expression was decreased after treatment with exosomes obtained from naive patients with IPF compared with control subjects (Figure 6F). However, its levels were higher after incubation with exosomes obtained from individuals with IPF taking nintedanib compared with naive patients with IPF or patients on pirfenidone. Interestingly, these results negatively correlated with miR-143-5p and miR-342-5p levels in exosomes (Figure 6A). FASN and ACSL-4 expressions were also decreased in naive patients with IPF compared with controls. However, FASN levels increased after ATII cell treatment with exosomes isolated from individuals taking pirfenidone or nintedanib compared with naive patients with IPF. Our results suggest the exosome-mediated effect of antifibrotic medications on ATII cells.

Next, we analyzed *SP-C*, *FASN*, and *ACSL-4* mRNA levels in ATII cells treated with exosomes obtained from naive patients with IPF and patients taking pirfenidone or nintedanib (Figure 6G). We found their increase only in ATII cells incubated with exosomes obtained from patients with IPF on nintedanib compared with naive patients with IPF. Also, SP-C expression was higher in ATII cells treated with exosomes isolated from individuals with IPF taking nintedanib than pirfenidone.

Interestingly, we detected a decrease in *SMAD3*, *CTGF*, *COL3A1*, and *TGFβ1* mRNA levels in control cultured fibroblasts treated with exosomes obtained from patients taking nintedanib compared with naive patients with IPF (Figure 6H). In addition, *SMAD3* expression was lower in fibroblasts treated with exosomes obtained from patients on pirfenidone than in naive patients with IPF. Treatment of fibroblasts with lung-derived exosomes obtained from individuals with IPF taking nintedanib decreased miR-143-5p and increased miR-342-5p levels compared with naive patients with IPF (Figure E6, Panel II, A). *ACSL-4* mRNA expression was higher in these patients in comparison with cell treatment with exosomes obtained from naive patients with IPF and pirfenidone-medicated patients with IPF; however, *FASN* levels were unchanged (Figure E6, Panel II, B). We did not detect any differences between FASN and ACSL-4 protein expression in fibroblasts treated with exosomes compared with controls by Western blotting (Figure E6, Panel II, C and D).

We examined the impact of lung tissue–derived exosomes obtained from control subjects, naive patients with IPF, or patients taking pirfenidone or nintedanib on ATII cell senescence and expression of factors related to Senescence-Associated

Secretory Phenotype (SASP). Cultured ATII cells isolated from control organ donors were used for treatment with exosomes. Our results indicate increased *P53*, *P16*, *P21*, and *IL-6* mRNA levels in ATII cells incubated with exosomes from naive patients with IPF compared with control subjects as detected by RT-PCR (Figure 6I). Exosomes obtained from patients with IPF taking pirfenidone or nintedanib lowered *P16*, *P21*, and *IL-6* levels compared with naive patients with IPF. Moreover, treatment with nintedanib also decreased *P53* expression. We found higher p-P53, P16, and P21 expression in cultured ATII cells incubated with exosomes obtained from naive patients with IPF than control subjects as detected by immunofluorescence (Figures 6J–6M). These results suggest that exosomes derived from lung tissue obtained from naive patients with IPF contribute to ATII cell senescence. Moreover, treatment of control ATII cells with exosomes obtained from patients taking nintedanib decreased p-P53, P16, and P21 levels compared with naive patients with IPF. To confirm the prosenescent effect of exosomes from naive patients with IPF, we used senescence-associated β-galactosidase (SA-β-Gal) staining. It was increased in control cultured ATII cells treated with exosomes obtained from naive patients with IPF compared with control organ donors (Figures 6N and 6O). Consistent with the previous data, SA-β-Gal was decreased after ATII cell treatment with exosomes obtained from patients with IPF medicated with nintedanib or pirfenidone. However, lower SA-β-Gal staining was detected in cells treated with exosomes obtained from patients with IPF on nintedanib compared with pirfenidone. Our results indicate that IPF treatment with pirfenidone and nintedanib may alter ATII cell function via exosomes and suggest an inhibitory effect of antifibrotic medications on IPF exosome-mediated ATII cell senescence. Also, control exosomes may decrease the profibrotic features of fibroblasts and provide a rescue. Further studies are required to determine the antifibrotic mechanism of these medications.

Discussion

Alteration of the repair capacity of alveolar epithelial cells induced by a chronic lung tissue injury is an early event in IPF (28). It relates to impaired alveolar epithelium regeneration due to ATII cell dysfunction. Exosomes can deliver their content, which depends on their cell of origin, to the recipient cells and are implicated in pathophysiological processes and diseases (29, 30). Studies described divergences in the effects of exosomes, which may be explained by tissue-specific effects. miRNAs are present in secreted and circulating exosomes (31). It has been reported that miRNAs can regulate 30–80% of the genes in the human genome (32, 33). They are also potential molecular targets for many diseases, including IPF. However, the impact of exosomal miRNAs on human primary ATII cells in this disease's development and progression is not well known.

We identified dysregulated miRNAs in exosomes in IPF. A high abundance of miR10A-5p was found, and its role as a potential biomarker in lung diseases was suggested (34, 35). Our results indicated that miR-143-5p and miR-342-5p are upregulated in ATII cells, lung tissue, plasma, and exosomes in naive patients with IPF compared with control organ donors. Because exosomes can contribute to cell–cell communication, we investigated their role in cultured ATII cells and fibroblasts. We treated control ATII cells and fibroblasts with IPF lung tissue–derived exosomes. We found that they negatively affected the *de novo* fatty acid synthesis pathway in ATII cells and increased the profibrotic response in fibroblasts. Fatty acid signaling has been shown to play a critical role in the pathogenesis and exacerbation of bleomycin-induced pulmonary fibrosis in mice (36). Moreover, our *in silico* analysis suggests that miR-143-5p and miR-342-5p target *FASN* and *ACSL-4*, key enzymes in this pathway. ACSL-4 is a long-chain fatty acyl-CoA synthetase, a key enzyme in regulating lipid composition and required to maintain phospholipid content (37, 38). Decreased lipid content, phospholipid biogenesis, and ACSL-4 levels contributed to poor cell survival and proliferation (39). We found lower FASN and ACSL-4 expression in ATII cells in IPF, associated with increased miR-143-5p and miR-342-5p levels. We overexpressed these miRNAs in control cultured ATII cells and fibroblasts and found downregulation of FASN and ACSL-4.

Inhibition of FASN is involved in cell cycle arrest and death (40, 41), and our data suggest its critical role in ATII cell dysfunction in IPF. It has been reported that inhibiting FASN activity by pharmacological agents or siRNA decreased cancer cell proliferation and induced apoptosis (42, 43). AMPK can also regulate FASN and associated metabolic processes (44). Pharmacological activation of AMPK in myofibroblasts in IPF displays lower fibrotic activity, together with enhanced mitochondrial biogenesis and normalization of sensitivity to apoptosis (45). Studies indicated that FASN is expressed in alveolar epithelial cells and regulated lipid synthesis (46, 47). Importantly, exposure of $Fasn^{i\Delta AEC2}$ mice to bleomycin increased lung fibrosis compared with control mice (46). In agreement with these data, our results suggest defective FASN-mediated lipid metabolism in ATII cells in patients with IPF.

Our results showed that treatment of control fibroblasts with exosomes obtained from naive patients with IPF increased *SMAD3*, *CTGF*, *COL3A1*, and *TGFβ1* mRNA expression, important mediators in IPF (48–50). In addition, we detected that exosomes obtained from severe IPF had higher miR-143-5p and miR-342-5p levels compared with areas with mild fibrosis. The same correlation was observed in control fibroblasts treated with these exosomes, which was associated with increased profibrotic gene expression. We thus favor the hypothesis that IPF-derived exosomes could stimulate profibrotic properties, leading to disease progression through miRNA-mediated mechanisms.

We found that exosomes from naive patients with IPF increased *IL-6*, *P53*, *P21*, and *P16* mRNA and p-P53, P16, and P21 protein expression in ATII cells and increased the number of SA-β-Gal+ ATII cells compared with control subjects. This indicates the proinflammatory response and DNA damage. Cell senescence is one of the characteristics of the altered reparative capacity of ATII cells (51). Our results suggest that the downregulation of FASN protein expression by exosomal miR-143-5p and miR-342-5p in ATII cells may contribute to their senescence. It was reported that P16- and P21-positive cells were found in the alveolar epithelium of IPF lungs, mainly in proSP-C+ KRT7+ ATII cells (52). We have shown that ATII cell senescence in IPF may impair their self-renewal and differentiation to alveolar type I cells (17). This indicates the critical role of exosomes in modulating ATII cell function in this disease.

The mechanism of action of pirfenidone and nintedanib is still poorly understood (3). We found decreased profibrotic response in control fibroblasts treated with exosomes obtained from lung tissue of patients with

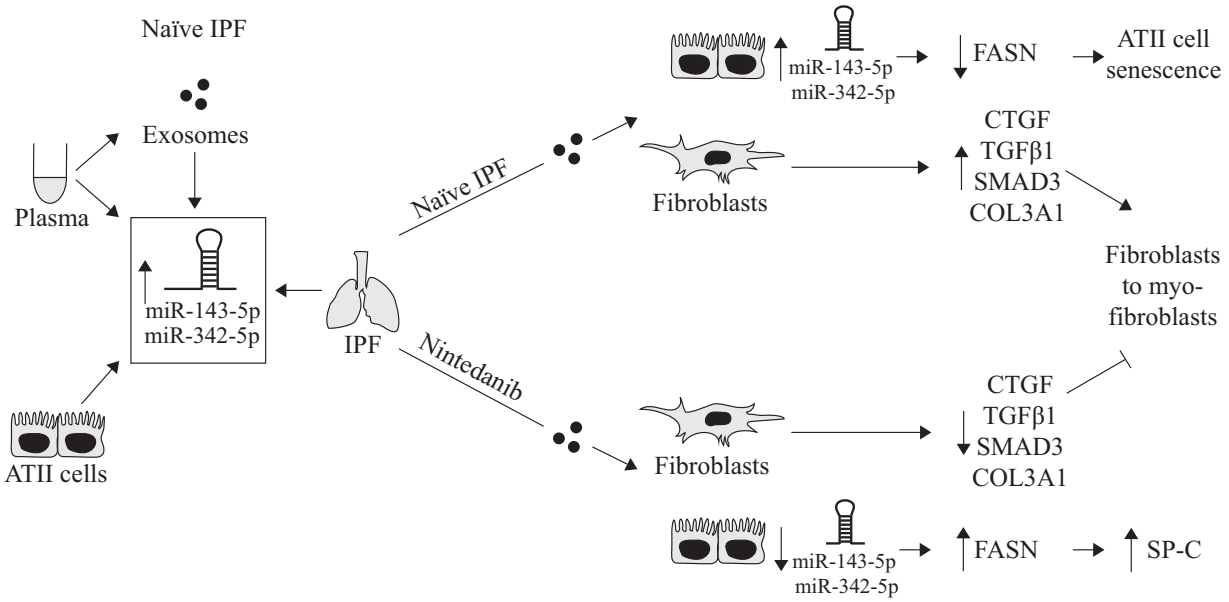

Figure 7. Model of the exosomal miRNA function in IPF. Increased miR-143-5p and miR-342-5p were detected in all analyzed samples obtained from naive patients with IPF. Lung tissue–derived exosomes isolated from naive patients with IPF induced ATII cell senescence and fibroblast differentiation to myofibroblasts. Exosomes obtained from patients with IPF treated with nintedanib increased SP-C expression in ATII cells and decreased expression of profibrotic genes in fibroblasts compared with naive patients with IPF.

IPF taking these drugs compared with exosomes isolated from naive patients with IPF. This suggests that these antifibrotic medications can modulate exosomes' content and alter recipient cells' function. Furthermore, we showed increased SP-C levels in ATII cells treated with exosomes isolated from patients with IPF taking nintedanib compared with naive patients with IPF. This indicates the beneficial effect of these drugs on the restoration of ATII cell function. It is worth noticing that ATII cells can inhibit fibroblast proliferation (53). Also, nintedanib and pirfenidone have different mechanisms of action (54). This can explain other observed differences in cell responses.

We also isolated exosomes from control organ donors. Given that exosomes differ in function depending on their origin (55), we analyzed their effect on fibroblasts isolated from naive patients with IPF. Interestingly, we found that this treatment decreased their profibrotic phenotype as detected by reduced *SMAD3*, *CTGF*, *COL3A1*, and *TGFβ1* mRNA expression in the recipient fibroblasts. Our results suggest that control exosomes may have potential therapeutic applications. Notably, mesenchymal stem cell–derived exosomes prevented and reverted experimental pulmonary fibrosis in mice (56). Also, potential beneficial effects of intratracheal transplantation of ATII cells obtained from organ donors in patients with IPF were reported (6).

In summary, our study reveals an impact of IPF-derived exosomes on human control primary ATII cells and fibroblasts (Figure 7). Moreover, we demonstrated the critical role of miR-143-5p and miR-342-5p in IPF. Our results suggest their contribution to fibrogenesis in disease pathogenesis and progression by transcriptional downregulation of the *de novo* fatty acid synthesis pathway. Targeting these miRNAs may restore ATII cell function as a novel strategy in IPF. ■

Author disclosures are available with the text of this article at www.atsjournals.org.

Acknowledgment: The authors thank Dr. Enkhee Purev for suggestions regarding PKH67 staining and Rohan Brebion for assistance. Lung tissue was provided through Temple Biobank (Temple University).

References

1. Raghu G, Remy-Jardin M, Myers JL, Richeldi L, Ryerson CJ, Lederer DJ, *et al.*; American Thoracic Society, European Respiratory Society, Japanese Respiratory Society, and Latin American Thoracic Society. Diagnosis of idiopathic pulmonary fibrosis: an official ATS/ERS/JRS/ALAT clinical practice guideline. *Am J Respir Crit Care Med* 2018;198: e44–e68.
2. Sharif R. Overview of idiopathic pulmonary fibrosis (IPF) and evidence-based guidelines. *Am J Manag Care* 2017;23:S176–S182.
3. Marijic P, Schwarzkopf L, Schwettmann L, Ruhnke T, Trudzinski F, Kreuter M. Pirfenidone vs. nintedanib in patients with idiopathic pulmonary fibrosis: a retrospective cohort study. *Respir Res* 2021;22:268.
4. Lin CR, Bahmed K, Kosmider B. Impaired alveolar re-epithelialization in pulmonary emphysema. *Cells* 2022;11:2055.
5. Parimon T, Yao C, Stripp BR, Noble PW, Chen P. Alveolar epithelial type II cells as drivers of lung fibrosis in idiopathic pulmonary fibrosis. *Int J Mol Sci* 2020;21:2269.
6. Serrano-Mollar A, Gay-Jordi G, Guillamat-Prats R, Closa D, Hernandez-Gonzalez F, Marin P, *et al.*; Pneumocyte Study Group. Safety and tolerability of alveolar type II cell transplantation in idiopathic pulmonary fibrosis. *Chest* 2016;150:533–543.
7. Doyle LM, Wang MZ. Overview of extracellular vesicles, their origin, composition, purpose, and methods for exosome isolation and analysis. *Cells* 2019;8:727.
8. Qiu Y, Li P, Zhang Z, Wu M. Insights into exosomal non-coding RNAs sorting mechanism and clinical application. *Front Oncol* 2021;11:664904.

9. Wang W, Zhu N, Yan T, Shi YN, Chen J, Zhang CJ, *et al.* The crosstalk: exosomes and lipid metabolism. *Cell Commun Signal* 2020;18:119.
10. Yang Y, Huang H, Li Y. Roles of exosomes and exosome-derived miRNAs in pulmonary fibrosis. *Front Pharmacol* 2022;13:928933.
11. Ramírez-Hernández AA, Velázquez-Enríquez JM, Santos-Álvarez JC, López-Martínez A, Reyes-Jiménez E, Carrasco-Torres G, *et al.* The role of extracellular vesicles in idiopathic pulmonary fibrosis progression: an approach on their therapeutics potential. *Cells* 2022;11:630.
12. Kadota T, Fujita Y, Araya J, Watanabe N, Fujimoto S, Kawamoto H, *et al.* Human bronchial epithelial cell-derived extracellular vesicle therapy for pulmonary fibrosis via inhibition of TGF-β-WNT crosstalk. *J Extracell Vesicles* 2021;10:e12124.
13. Kadota T, Yoshioka Y, Fujita Y, Araya J, Minagawa S, Hara H, *et al.* Extracellular vesicles from fibroblasts induce epithelial-cell senescence in pulmonary fibrosis. *Am J Respir Cell Mol Biol* 2020;63:623–636.
14. Yang M, Tang X, Wang Z, Wu X, Tang D, Wang D. miR-125 inhibits colorectal cancer proliferation and invasion by targeting TAZ. *Biosci Rep* 2019;39:BSR20190193.
15. Stolzenburg LR, Harris A. The role of microRNAs in chronic respiratory disease: recent insights. *Biol Chem* 2018;399:219–234.
16. Rajasekaran S, Rajaguru P, Sudhakar Gandhi PS. MicroRNAs as potential targets for progressive pulmonary fibrosis. *Front Pharmacol* 2015;6:254.
17. Moimas S, Salton F, Kosmider B, Ring N, Volpe MC, Bahmed K, *et al.* miR-200 family members reduce senescence and restore idiopathic pulmonary fibrosis type II alveolar epithelial cell transdifferentiation. *ERJ Open Res* 2019;5:00138-2019.
18. Mashima T, Seimiya H, Tsuruo T. De novo fatty-acid synthesis and related pathways as molecular targets for cancer therapy. *Br J Cancer* 2009;100:1369–1372.
19. Humbert M, Seiler K, Mosimann S, Rentsch V, Sharma K, Pandey AV, *et al.* Reducing FASN expression sensitizes acute myeloid leukemia cells to differentiation therapy. *Cell Death Differ* 2021;28:2465–2481.
20. Jones SF, Infante JR. Molecular pathways: fatty acid synthase. *Clin Cancer Res* 2015;21:5434–5438.
21. Ates G, Goldberg J, Currais A, Maher P. CMS121, a fatty acid synthase inhibitor, protects against excess lipid peroxidation and inflammation and alleviates cognitive loss in a transgenic mouse model of Alzheimer's disease. *Redox Biol* 2020;36:101648.
22. Plataki M, Fan L, Sanchez E, Huang Z, Torres LK, Imamura M, *et al.* Fatty acid synthase downregulation contributes to acute lung injury in murine diet-induced obesity. *JCI Insight* 2019;5:e127823.
23. Fafián-Labora J, Carpintero-Fernández P, Jordan SJD, Shikh-Bahaei T, Abdullah SM, Mahenthiran M, *et al.* FASN activity is important for the initial stages of the induction of senescence. *Cell Death Dis* 2019;10:318.
24. Kosmider B, Mason RJ, Bahmed K. Isolation and characterization of human alveolar type II cells. *Methods Mol Biol* 2018;1809:83–90.
25. Pratte KA, Curtis JL, Kechris K, Couper D, Cho MH, Silverman EK, *et al.* Soluble receptor for advanced glycation end products (sRAGE) as a biomarker of COPD. *Respir Res* 2021;22:127.
26. Livshits MA, Khomyakova E, Evtushenko EG, Lazarev VN, Kulemin NA, Semina SE, *et al.* Isolation of exosomes by differential centrifugation: theoretical analysis of a commonly used protocol. *Sci Rep* 2015;5:17319.
27. Drury J, Rychahou PG, He D, Jafari N, Wang C, Lee EY, *et al.* Inhibition of fatty acid synthase upregulates expression of CD36 to sustain proliferation of colorectal cancer cells. *Front Oncol* 2020;10:1185.
28. Wu H, Yu Y, Huang H, Hu Y, Fu S, Wang Z, *et al.* Progressive pulmonary fibrosis is caused by elevated mechanical tension on alveolar stem cells. *Cell* 2020;180:107–121.e17.
29. Ding H, Li LX, Harris PC, Yang J, Li X. Extracellular vesicles and exosomes generated from cystic renal epithelial cells promote cyst growth in autosomal dominant polycystic kidney disease. *Nat Commun* 2021;12:4548.
30. Melo SA, Luecke LB, Kahlert C, Fernandez AF, Gammon ST, Kaye J, *et al.* Glypican-1 identifies cancer exosomes and detects early pancreatic cancer. *Nature* 2015;523:177–182.
31. Bhome R, Del Vecchio F, Lee GH, Bullock MD, Primrose JN, Sayan AE, *et al.* Exosomal microRNAs (exomiRs): small molecules with a big role in cancer. *Cancer Lett* 2018;420:228–235.
32. Lu J, Clark AG. Impact of microRNA regulation on variation in human gene expression. *Genome Res* 2012;22:1243–1254.
33. Cadena-Suárez AR, Hernández-Hernández HA, Alvarado-Vásquez N, Rangel-Escareño C, Sommer B, Negrete-García MC. Role of microRNAs in signaling pathways associated with the pathogenesis of idiopathic pulmonary fibrosis: a focus on epithelial-mesenchymal transition. *Int J Mol Sci* 2022;23:6613.
34. Tsai MJ, Tsai YC, Chang WA, Lin YS, Tsai PH, Sheu CC, *et al.* Deducting microRNA-mediated changes common in bronchial epithelial cells of asthma and chronic obstructive pulmonary disease-a next-generation sequencing-guided bioinformatic approach. *Int J Mol Sci* 2019;20:553.
35. Bao M, Pan S, Yang W, Chen S, Shan Y, Shi H. Serum miR-10a-5p and miR-196a-5p as non-invasive biomarkers in non-small cell lung cancer. *Int J Clin Exp Pathol* 2018;11:773–780.
36. Sunaga H, Matsui H, Ueno M, Maeno T, Iso T, Syamsunarno MR, *et al.* Deranged fatty acid composition causes pulmonary fibrosis in Elovl6-deficient mice. *Nat Commun* 2013;4:2563.
37. Kuwata H, Hara S. Role of acyl-CoA synthetase ACSL4 in arachidonic acid metabolism. *Prostaglandins Other Lipid Mediat* 2019;144:106363.
38. Ji Q, Fu S, Zuo H, Huang Y, Chu L, Zhu Y, *et al.* ACSL4 is essential for radiation-induced intestinal injury by initiating ferroptosis. *Cell Death Discov* 2022;8:332.
39. Li YJ, Fahrmann JF, Aftabizadeh M, Zhao Q, Tripathi SC, Zhang C, *et al.* Fatty acid oxidation protects cancer cells from apoptosis by increasing mitochondrial membrane lipids. *Cell Rep* 2022;39:111044.
40. Zhang W, Huang J, Tang Y, Yang Y, Hu H. Inhibition of fatty acid synthase (FASN) affects the proliferation and apoptosis of HepG2 hepatoma carcinoma cells via the β-catenin/C-myc signaling pathway. *Ann Hepatol* 2020;19:411–416.
41. Zecchin KG, Rossato FA, Raposo HF, Melo DR, Alberici LC, Oliveira HC, *et al.* Inhibition of fatty acid synthase in melanoma cells activates the intrinsic pathway of apoptosis. *Lab Invest* 2011;91:232–240.
42. Alwarawrah Y, Hughes P, Loiselle D, Carlson DA, Darr DB, Jordan JL, *et al.* Fasnall, a selective FASN inhibitor, shows potent anti-tumor activity in the MMTV-Neu model of HER2(+) breast cancer. *Cell Chem Biol* 2016;23:678–688.
43. Flavin R, Peluso S, Nguyen PL, Loda M. Fatty acid synthase as a potential therapeutic target in cancer. *Future Oncol* 2010;6:551–562.
44. Luo Z, Zang M, Guo W. AMPK as a metabolic tumor suppressor: control of metabolism and cell growth. *Future Oncol* 2010;6:457–470.
45. Rangarajan S, Bone NB, Zmijewska AA, Jiang S, Park DW, Bernard K, *et al.* Metformin reverses established lung fibrosis in a bleomycin model. *Nat Med* 2018;24:1121–1127.
46. Chung KP, Hsu CL, Fan LC, Huang Z, Bhatia D, Chen YJ, *et al.* Mitofusins regulate lipid metabolism to mediate the development of lung fibrosis. *Nat Commun* 2019;10:3390.
47. Treutlein B, Brownfield DG, Wu AR, Neff NF, Mantalas GL, Espinoza FH, *et al.* Reconstructing lineage hierarchies of the distal lung epithelium using single-cell RNA-seq. *Nature* 2014;509:371–375.
48. Yang F, Hou ZF, Zhu HY, Chen XX, Li WY, Cao RS, *et al.* Catalpol protects against pulmonary fibrosis through inhibiting TGF- β1/Smad3 and Wnt/β-catenin signaling pathways. *Front Pharmacol* 2021;11:594139.
49. Effendi WI, Nagano T. Connective tissue growth factor in idiopathic pulmonary fibrosis: breaking the bridge. *Int J Mol Sci* 2022;23:6064.
50. Vallée A, Lecarpentier Y. TGF-β in fibrosis by acting as a conductor for contractile properties of myofibroblasts. *Cell Biosci* 2019;9:98.
51. Rana T, Jiang C, Liu G, Miyata T, Antony V, Thannickal VJ, *et al.* PAI-1 regulation of TGF- β1-induced alveolar type II cell senescence, SASP secretion, and SASP-mediated activation of alveolar macrophages. *Am J Respir Cell Mol Biol* 2020;62:319–330.
52. Lehmann M, Korfei M, Mutze K, Klee S, Skronska-Wasek W, Alsafadi HN, *et al.* Senolytic drugs target alveolar epithelial cell function and attenuate experimental lung fibrosis *ex vivo*. *Eur Respir J* 2017;50:1602367.
53. Portnoy J, Pan T, Dinarello CA, Shannon JM, Westcott JY, Zhang L, *et al.* Alveolar type II cells inhibit fibroblast proliferation: role of IL-1alpha. *Am J Physiol Lung Cell Mol Physiol* 2006;290:L307–L316.
54. Finnerty JP, Ponnuswamy A, Dutta P, Abdelaziz A, Kamil H. Efficacy of antifibrotic drugs, nintedanib and pirfenidone, in treatment of progressive pulmonary fibrosis in both idiopathic pulmonary fibrosis (IPF) and non-IPF: a systematic review and meta-analysis. *BMC Pulm Med* 2021;21:411.
55. Rajagopal C, Harikumar KB. The origin and functions of exosomes in cancer. *Front Oncol* 2018;8:66.
56. Mansouri N, Willis GR, Fernandez-Gonzalez A, Reis M, Nassiri S, Mitsialis SA, *et al.* Mesenchymal stromal cell exosomes prevent and revert experimental pulmonary fibrosis through modulation of monocyte phenotypes. *JCI Insight* 2019;4:e128060.